Grant Number : 85-0033A

AFOSR-TR- 87-0446

INVESTIGATIONS ON LOCAL SEISMIC PHASES AND EVALUATION OF BODY WAVES MAGNITUDE (WESTERN EUROPE)

Principal Investigators : B. Massinon and P. Mechler

Redactors : B. Massinon and P. Mechler

RADIOMANA
Société Civile
27 Rue Claude Bernard
75005 Paris
FRANCE

January 1987

~~Annual Scientific Report~~, 1 December 1985 - 30 November 1986

Approved for public release : distribution unlimited

FINAL

Prepared for :

ADVANCED RESEARCH PROJECTS AGENCY (DOD)

and

EUROPEAN OFFICE AEROSPACE RESEARCH AND DEVELOPMENT

LONDON - ENGLAND

Sponsored by

Advanced Research Projects Agency (DOD)

DARPA Order N° 4493 9

Monitored by AFOSR / PKZ

Under Grant N° AFOSR 85-0033A

UNCLASSIFIED

SECURITY CLASSIFICATION OF THIS PAGE

REPORT DOCUMENTATION PAGE

1a. REPORT SECURITY CLASSIFICATION: Unclassified	1b. RESTRICTIVE MARKINGS
2a. SECURITY CLASSIFICATION AUTHORITY	3. DISTRIBUTION/AVAILABILITY OF REPORT: Approved for public release Distribution unlimited
2b. DECLASSIFICATION/DOWNGRADING SCHEDULE	
4. PERFORMING ORGANIZATION REPORT NUMBER(S)	5. MONITORING ORGANIZATION REPORT NUMBER(S): AFOSR-TR- 87-0446
6a. NAME OF PERFORMING ORGANIZATION: RADIOMANA Sté Civile; 6b. OFFICE SYMBOL (If applicable)	7a. NAME OF MONITORING ORGANIZATION: AFOSR / PKZA
6c. ADDRESS (City, State and ZIP Code): 27, rue Claude Bernard 75005 PARIS	7b. ADDRESS (City, State and ZIP Code): Building 410 Bolling AFB, DC 20332 - 6448
8a. NAME OF FUNDING/SPONSORING ORGANIZATION: ~~EOARD~~ AFOSR; 8b. OFFICE SYMBOL (If applicable): NP	9. PROCUREMENT INSTRUMENT IDENTIFICATION NUMBER: AFOSR 85 - 0033 A
8c. ADDRESS (City, State and ZIP Code): [redacted] same as 7b.	10. SOURCE OF FUNDING NOS. — PROGRAM ELEMENT NO.: 62714 E; PROJECT NO.: 4493; TASK NO.: 09; WORK UNIT NO.:
11. TITLE (Include Security Classification): Investigations on local seismic phases and evaluation of body waves magnitude (W. Europe)	
12. PERSONAL AUTHOR(S): B. MASSINON and P. MECHLER	
13a. TYPE OF REPORT: Final; 13b. TIME COVERED: FROM 01.12.85 TO 30.11.86	14. DATE OF REPORT (Yr., Mo., Day): 31.01.1987; 15. PAGE COUNT: 76
16. SUPPLEMENTARY NOTATION	
17. COSATI CODES — FIELD; GROUP; SUB. GR.	18. SUBJECT TERMS (Continue on reverse if necessary and identify by block number): Lg phase, Rg phase, Attenuation, Quality factor, Source function; Data processing; ~~Data base~~, ~~Synthetic sismogram~~, Seismic moment; Stress drop; Fault dimension; Western Europe

19. ABSTRACT (Continue on reverse if necessary and identify by block number)

During 1986, most of our efforts have concerned a better understanding of seismic sources and propagation on local and regional sismograms and m_b optimum determination The influence of source depth on local sismograms (10 - 60 km) has been carried on by using synthetics. Pg and Sg waves amplitudes are less influenced than Rg waves amplitudes by depth variations. Rg waves amplitudes are clearly decreasing when depth increases.

We need to apply such a discriminant on real cases.

A tomography method is used on Q Lg determination from regional seismic data over France area. A systematic Q computation on a large amount of data is necessary to have a reasonable statistical value.

For that purpose, a regional seismic data base including digital records and correspon-

20. DISTRIBUTION/AVAILABILITY OF ABSTRACT: UNCLASSIFIED/UNLIMITED ☐ SAME AS RPT. ☐ DTIC USERS ☐	21. ABSTRACT SECURITY CLASSIFICATION: UNCLASSIFIED
22a. NAME OF RESPONSIBLE INDIVIDUAL: JAN F. PRINCE	22b. TELEPHONE NUMBER (Include Area Code): (202) 767-4908; 22c. OFFICE SYMBOL: NP

DD FORM 1473, 83 APR — EDITION OF 1 JAN 73 IS OBSOLETE.

UNCLASSIFIED

SECURITY CLASSIFICATION OF THIS PAGE

ding seismic sources obtained by inversion technique (with a mean geometrical and anelastic attenuations) is actually prepared. About more than 400 earthquakes are processed, all of them located in France or in the vicinity at crustal depths.
Studies and processing concerning a better m_b evaluation on teleseisms recorded on a large network (L. D. G. network) are also continuing.

Grant Number : 85-0033A

INVESTIGATIONS ON LOCAL SEISMIC PHASES AND EVALUATION OF BODY WAVES MAGNITUDE (WESTERN EUROPE)

Principal Investigators : B. Massinon and P. Mechler
Redactors : B. Massinon and P. Mechler

R A D I O M A N A
Société Civile
27 Rue Claude Bernard
75005 Paris
FRANCE

January 1987
Annual Scientific Report, 1 December 1985 - 30 November 1986
Approved for public release : distribution unlimited

Prepared for :

ADVANCED RESEARCH PROJECTS AGENCY (DOD)
and
EUROPEAN OFFICE AEROSPACE RESEARCH AND DEVELOPMENT
LONDON - ENGLAND

Sponsored by
Advanced Research Projects Agency (DOD)
DARPA Order N° 4493 9
Monitored by AFOSR / PKZ
Under Grant N° AFOSR 85-0033A

THE VIEWS AND CONCLUSIONS CONTAINED IN THIS DOCUMENT ARE THOSE OF THE AUTHORS AND SHOULD NOT BE INTERPRETED AS NECESSARILY REPRESENTING THE OFFICIAL POLICIES, EITHER EXPRESSED OR IMPLIED, OF THE DEFENSE ADVANCED RESEARCH PROJECTS AGENCY OF THE U.S. GOVERNMENT.

TABLE OF CONTENTS

A - SOURCE DEPTH DETERMINATION AT LOCAL AND REGIONAL DISTANCES

B - INVERSION METHOD ON Q (f) - Q TOMOGRAPHY ON FRANCE AREA

C - SOURCE STUDIES - DATA BASE

D - PRESENTATIONS AT THE DARPA MEETING OF COLORADO SPRING - MAY 1986 -

A - SOURCE DEPTH DETERMINATION AT LOCAL AND REGIONAL DISTANCES

In a previous study (see Annual Scientific Report, year 1982) we tried to evaluate the influence of source depth on regional phases amplitudes recorded between 20 and 500 km of epicentral distances. For that purpose, synthetics were computed by the Bouchon method and Pg and Lg waves amplitudes were evaluated for various depths : 5, 17, 29, 31 km.

Besides attenuation's evaluation, it clearly appeared that Pg waves amplitudes are rather independant of depth and that Lg waves amplitudes are decreasing versus depth.

Our purpose this year is to evaluate if this method could help to discriminate events versus depth. We have started with local epicentral distances (10 to 60 km).

Method of synthetics computation

The method of synthetics is based on an exact discrete wave numbers computation (Bouchon 1982). We briefly recall that it allows to evaluate the total field representing the ground motion $\vec{S}(\omega)$ as :

$$\vec{S}(\omega) = \sum_{i=1}^{3} \sum_{j=1}^{3} M_{ij}(\omega) \; X_j(\omega) \; \vec{l}_i$$

in the frequency domain

with :

- $(\vec{l_i})_i$ = 1, 3 base

- M_{ij} 3x3 seismic moment tensor describing the slope of the source and the time history of rupture.
  This moment tensor M_{ij} is a product of two factors :
  - $s(\omega)$ describing the rupture versus time
  - m_{ij} scalare factor describing the source geometry (in our case a pure strike slope)

  One representation of the source function $s(\omega)$ is given by Brune :

$$s(\omega) \quad \frac{s(o)}{\sqrt{1 + (f/fc)^{2\alpha}}}$$

- $X_j(\omega)$ is representative of the propagation and depends on the epicentral distance, and the source depth.

The propagation model we have used defines a crust model for France (Darpa Annual Report, 1984) currently used. No anelastic attenuation has been taken into account ($Q = \infty$).
Different seismograms have been computed every 10 km of epicentral distance from 10 to 60 km, for different depths : 1, 3, 6, 9, 12 and 27 km within the crust.

Results

Computed impulse responses have been convolved by a source function of Brune type with a corner frequency fc = 3 Hz and an asymptote defined by $\alpha = 2$ (Fig. 1).
The evolution of signal with depth is clearly seen : very complicated with a source near the surface, essentially composed of guided waves in the

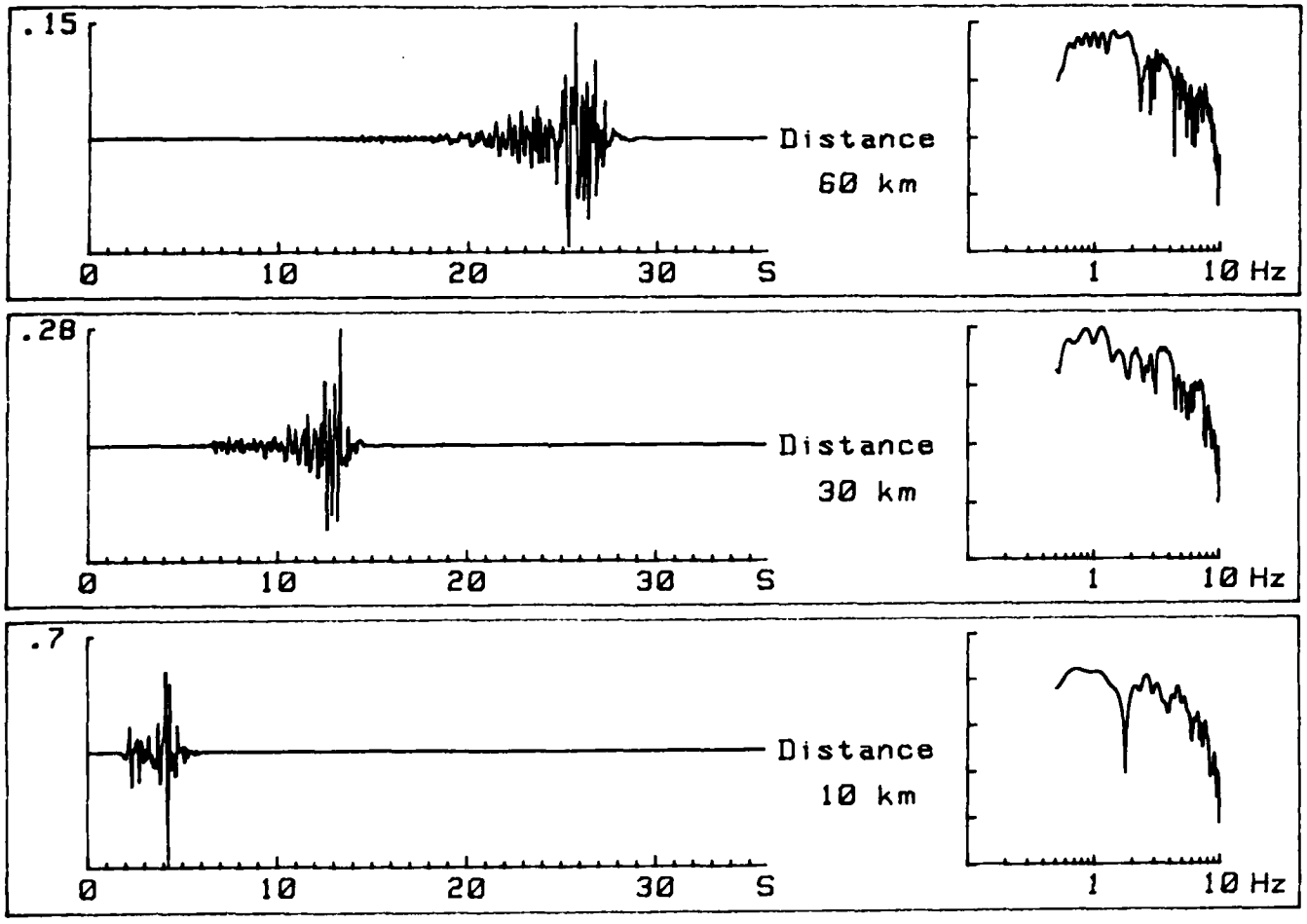

DEPTH: 1 km

Fig. 1-a - VELOCITY SYNTHETIC SISMOGRAMS AND CORRESPONDING DISPLACEMENT FREQUENCY SPECTRA

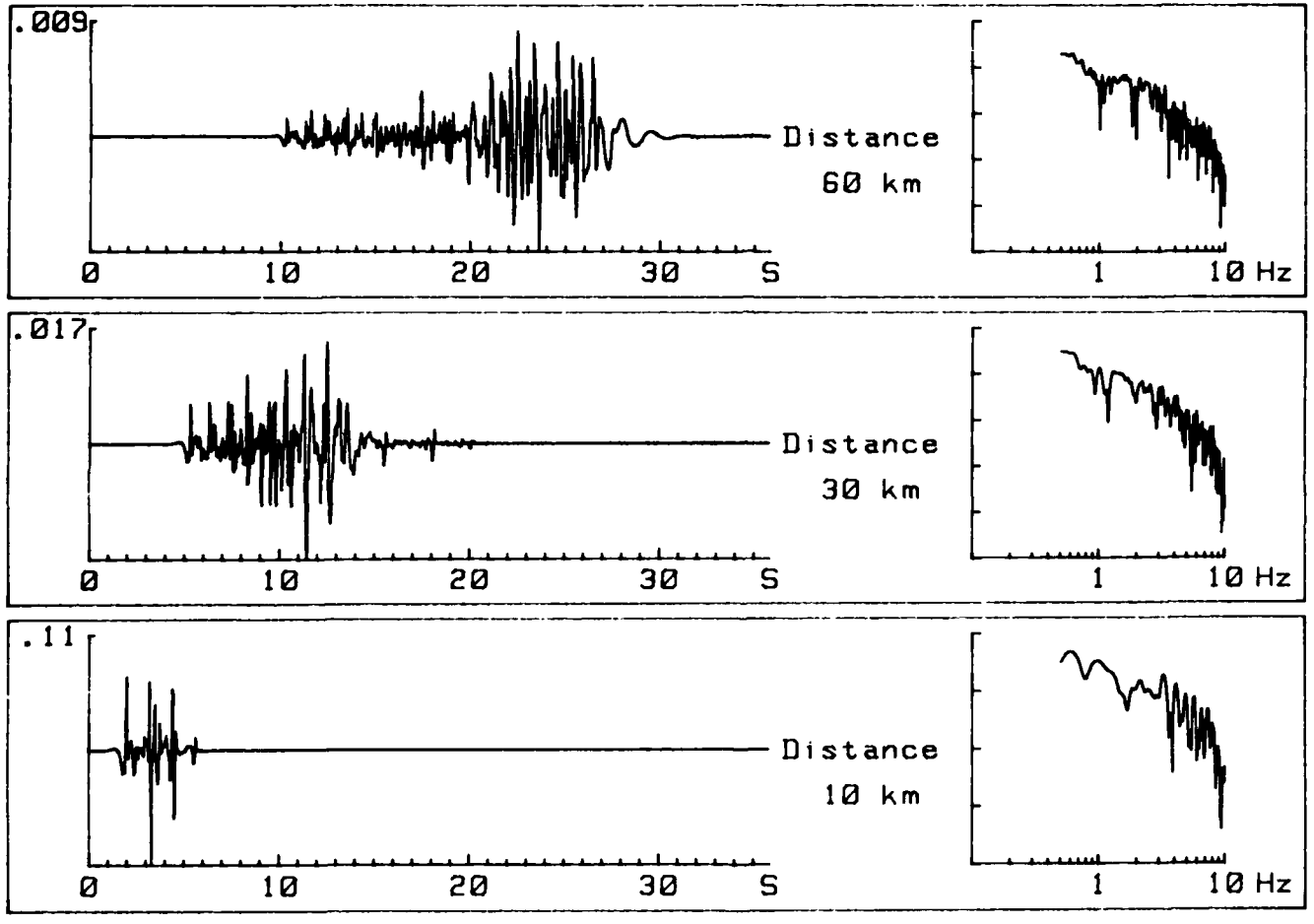

DEPTH: 3 km

Fig. 1-b - VELOCITY SYNTHETIC SEISMOGRAMS AND CORRESPONDING DISPLACEMENT FREQUENCY SPECTRA

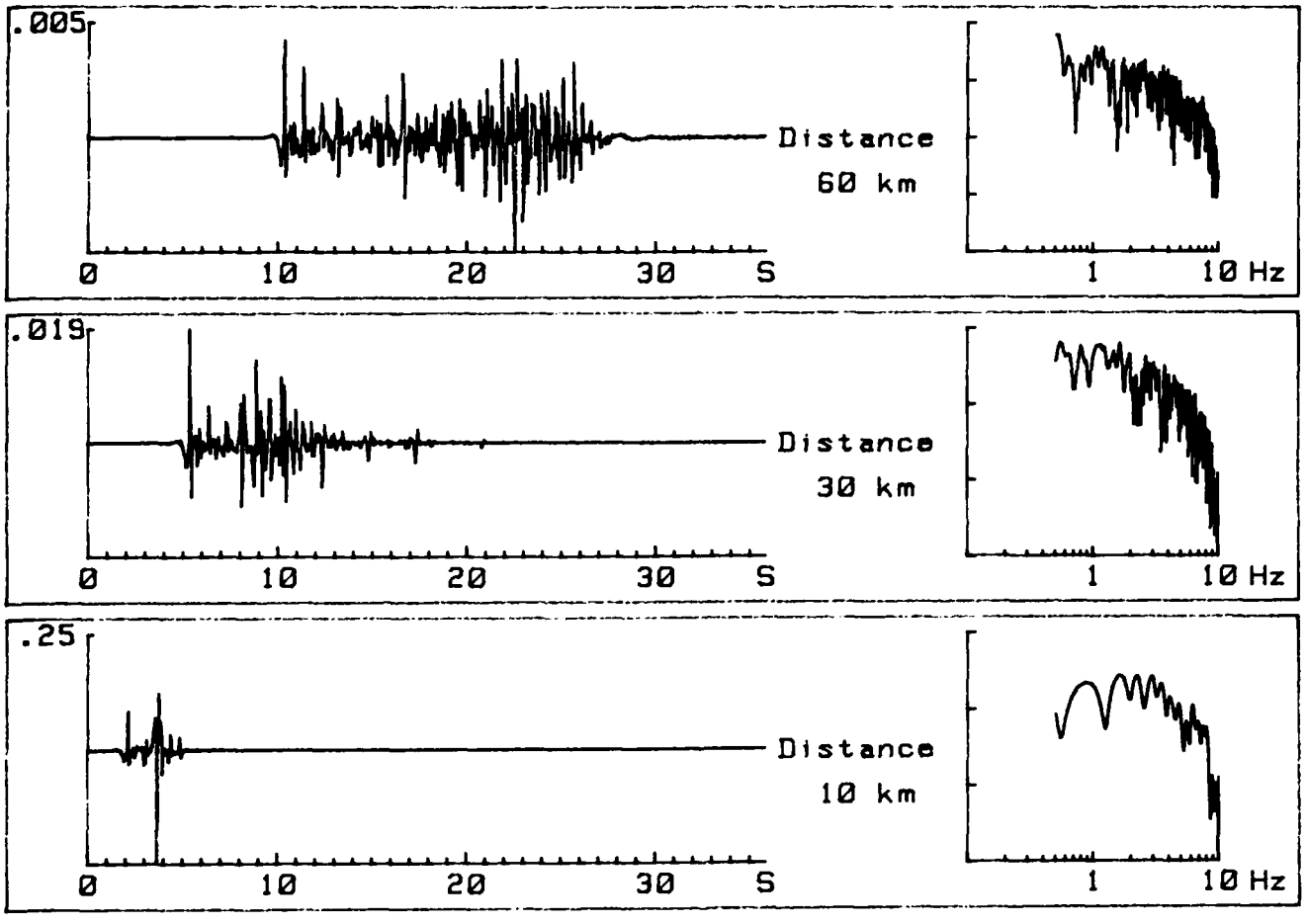

DEPTH: 6 km

Fig. 1-c - VELOCITY SYNTHETIC SISMOGRAMS AND CORRESPONDING DISPLACEMENT FREQUENCY SPECTRA

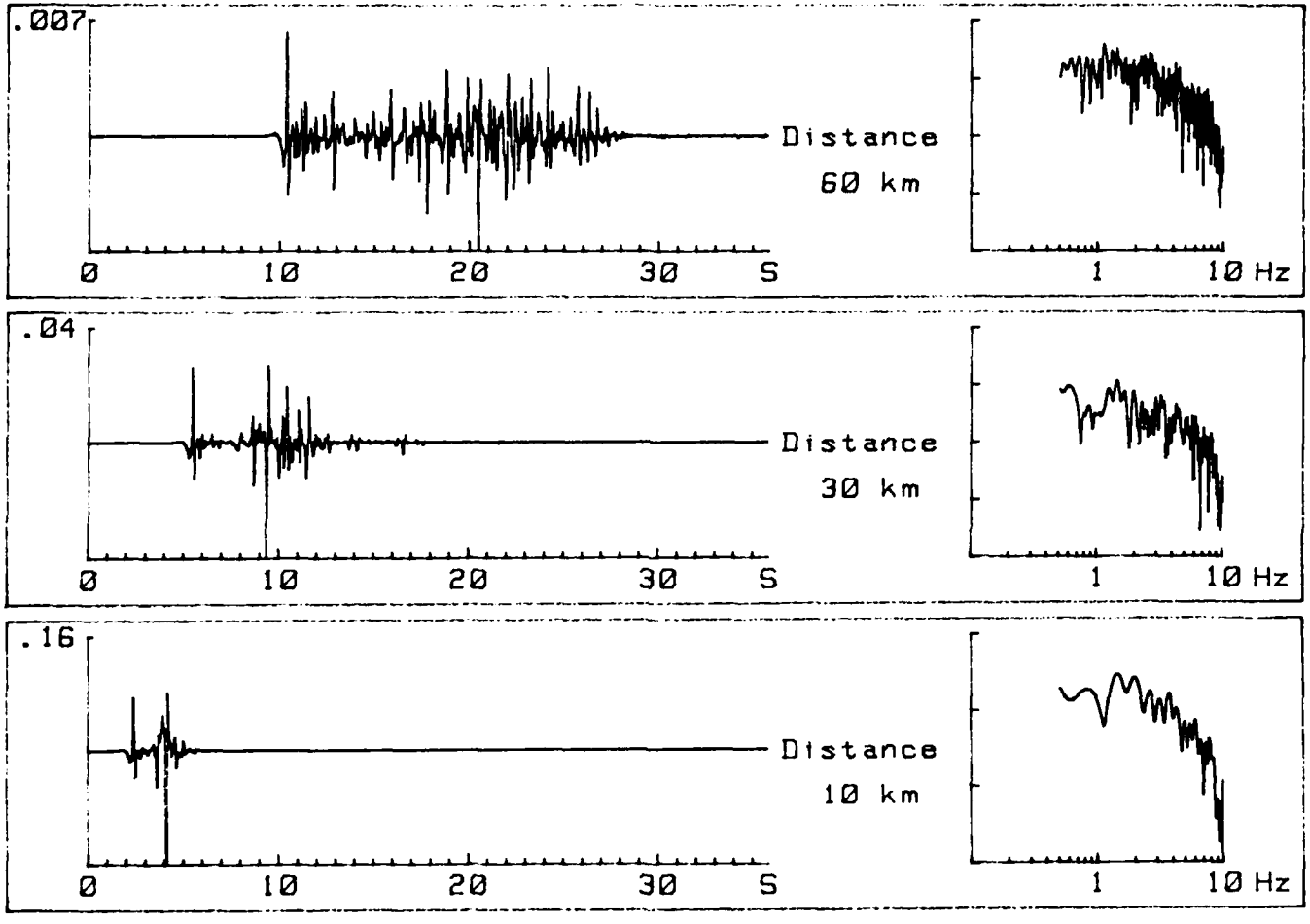

DEPTH: 9 km

Fig. 1-d - VELOCITY SYNTHETIC SISMOGRAMS AND CORRESPONDING DISPLACEMENT FREQUENCY SPECTRA

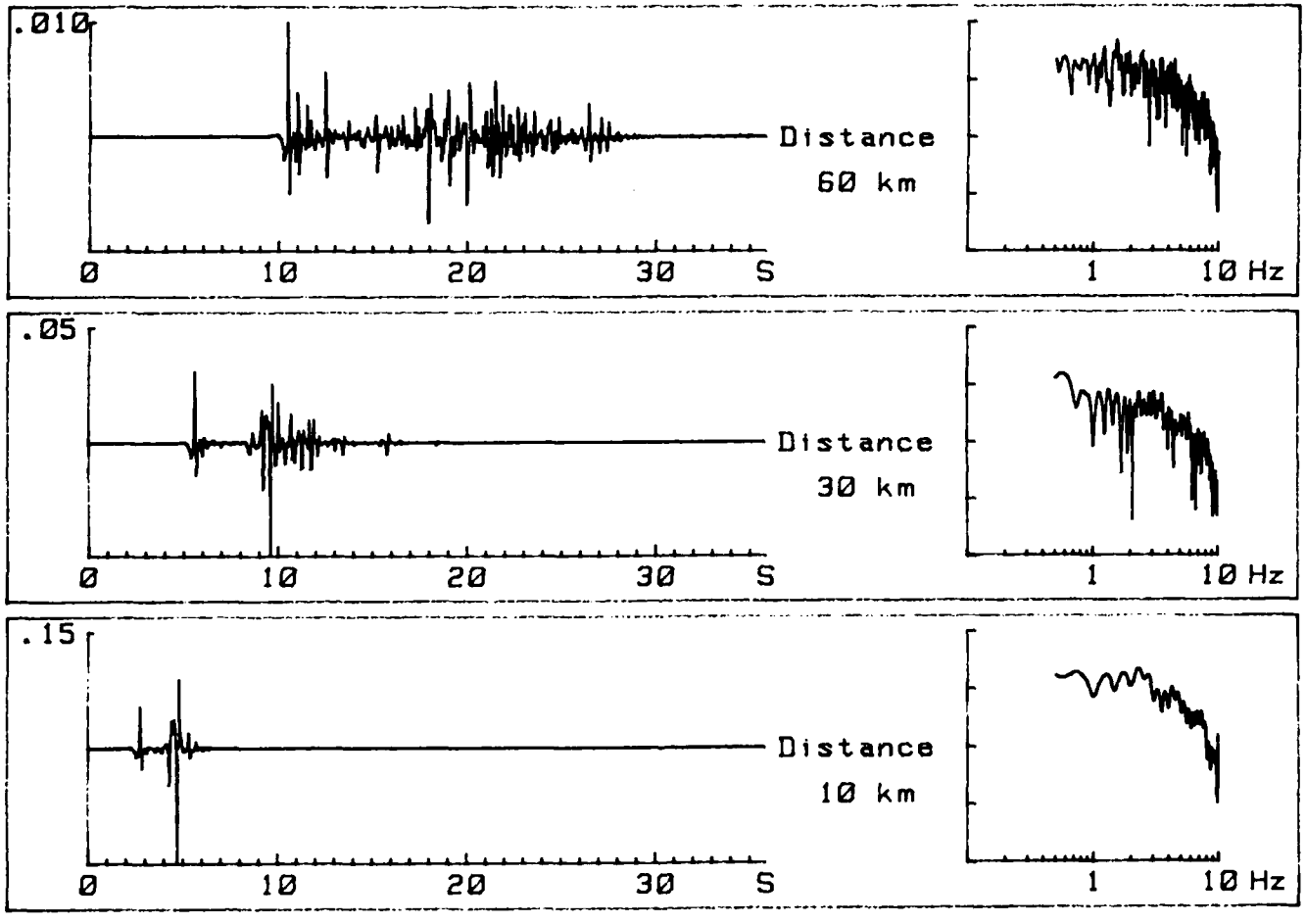

DEPTH: 12 km

Fig. 1-e - VELOCITY SYNTHETIC SISMOGRAMS AND CORRESPONDING DISPLACEMENT FREQUENCY SPECTRA

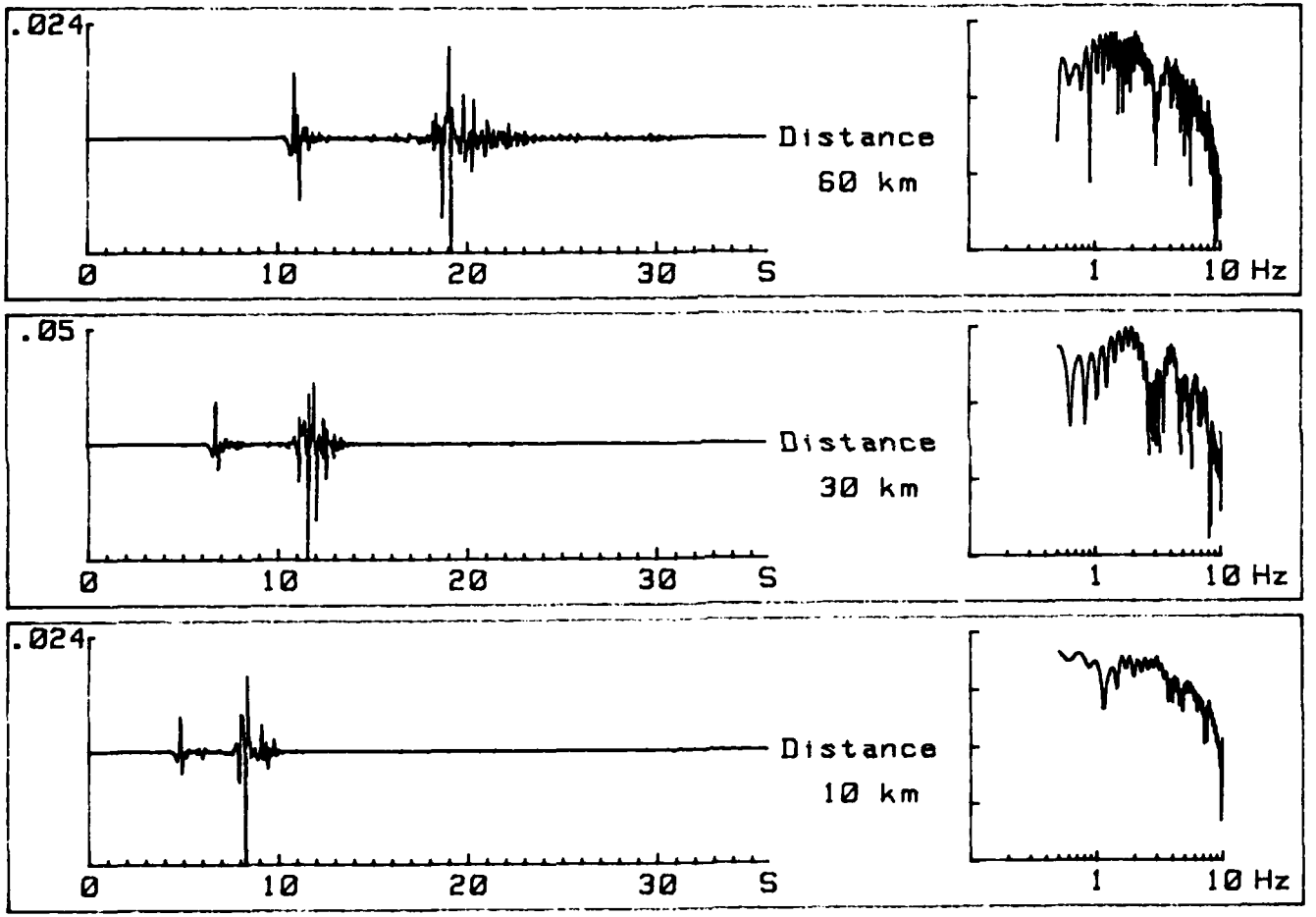

DEPTH: 27 km

Fig. 1-f - VELOCITY SYNTHETIC SISMOGRAMS AND CORRESPONDING DISPLACEMENT FREQUENCY SPECTRA

first layers, it becomes simpler and simpler versus depth : only direct P and S waves still exist.

In the frequency domain, this effect seems to be clearer.

We have computed amplitude spectra for :

- Pg phases (time window defined between V = 6,5km/s and 3,8km/s)
- Sg phases (" " " " V = 3,8km/s and 2,5km/s)
- Rg waves (" " " " V = 2,5km/s and 0,8km/s)

The computed spectra are shown on Fig. 2 (a, b, c, d, e, f) for distances rounding from 10 to 60 km.

Sg and particularly Pg phases are rather less influenced by depth except for very short distances. The Rg phases (surface waves in sedimentary layers) have their max. to min. spectral ratio ranging between 100 and 1 000. The effect of distance is clearly seen.

In order to be independant of this distance effect rough synthetics are deconvolved from geometrical attenuation.

Inversion of the source

Inversion technique is applied in the frequency domain to the synthetics to obtain simultaneously the source spectrum and the geometrical attenuation this being done on each phases for each distance and each depth previously selected.

Geometrical attenuation coefficients are largely increasing with depth for Sg waves from 1,25 (1 km) to 2,50 (6 km) and then rather independant (9 to 12 km).

For Pg waves, geometrical attenuation seems slightly dependant on depth, increasing from 1,70 (1 km) to 2,00 (6 km) and decreasing to 1,70 (12 km).

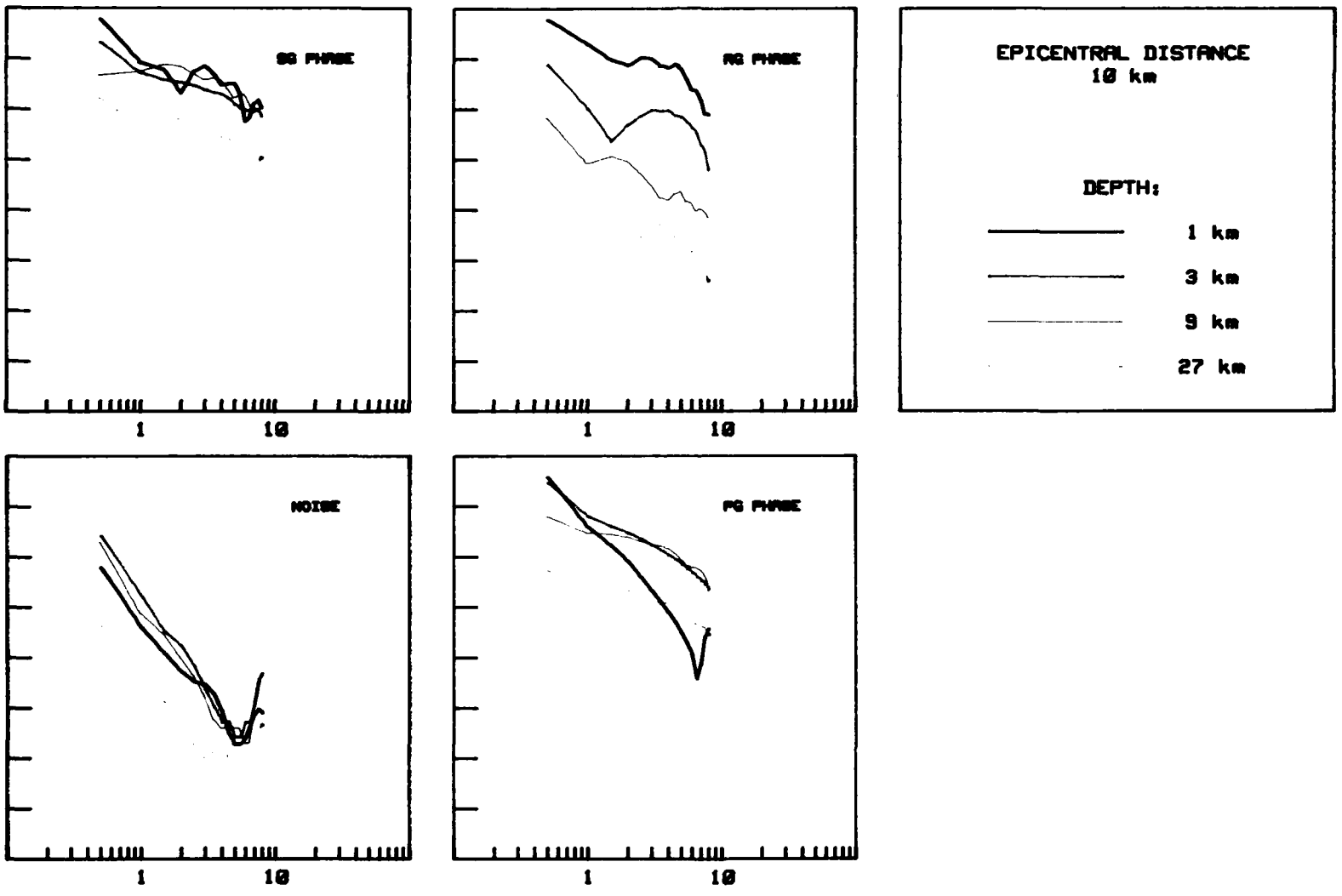

Fig. 2-a - SYNTHETIC DISPLACEMENT SPECTRA AT ONE EPICENTRAL DISTANCE FOR VARIOUS SOURCE DEPTHS

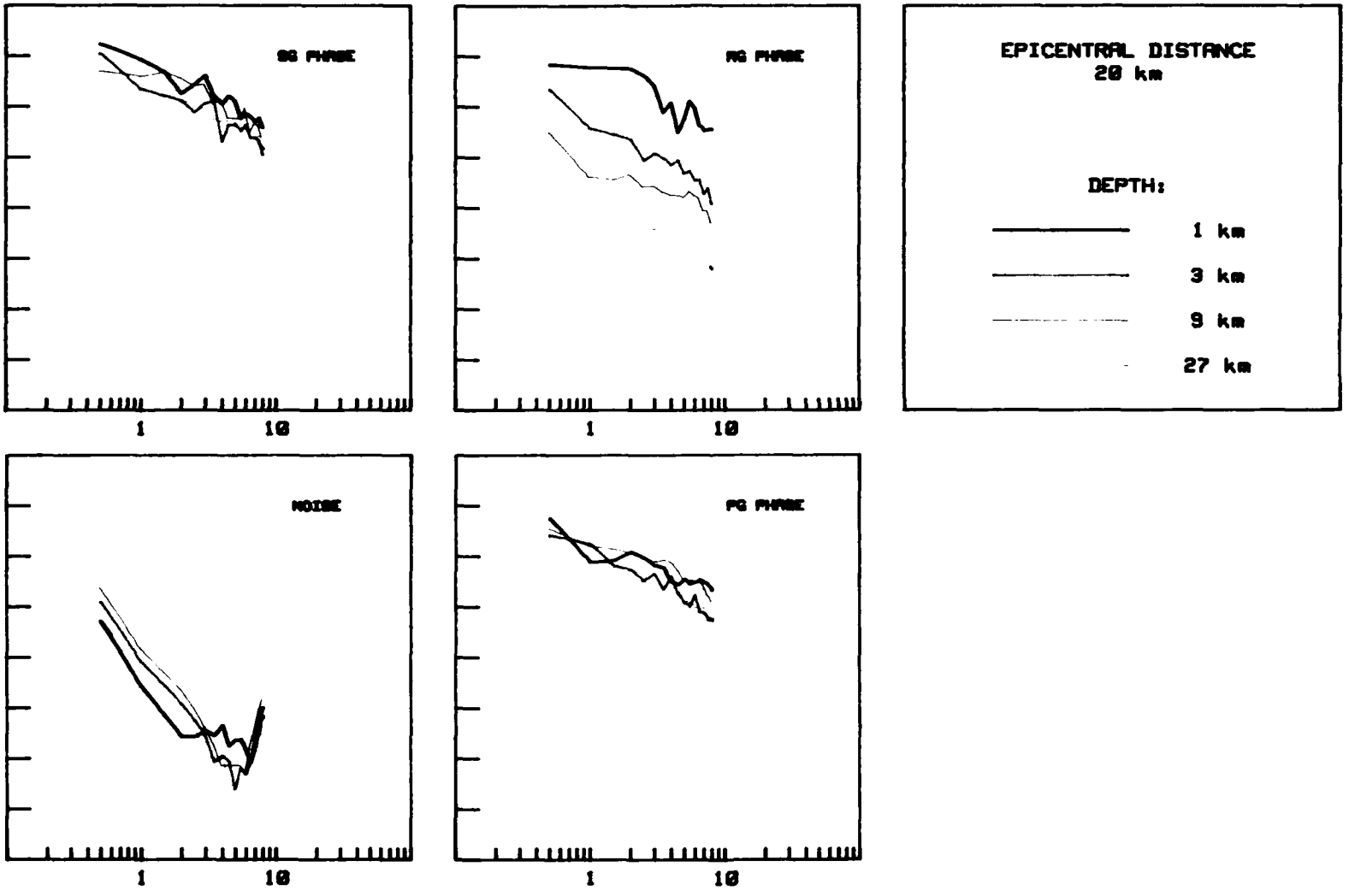

Fig. 2-b - SYNTHETIC DISPLACEMENT SPECTRA AT ONE EPICENTRAL DISTANCE FOR VARIOUS SOURCE DEPTHS

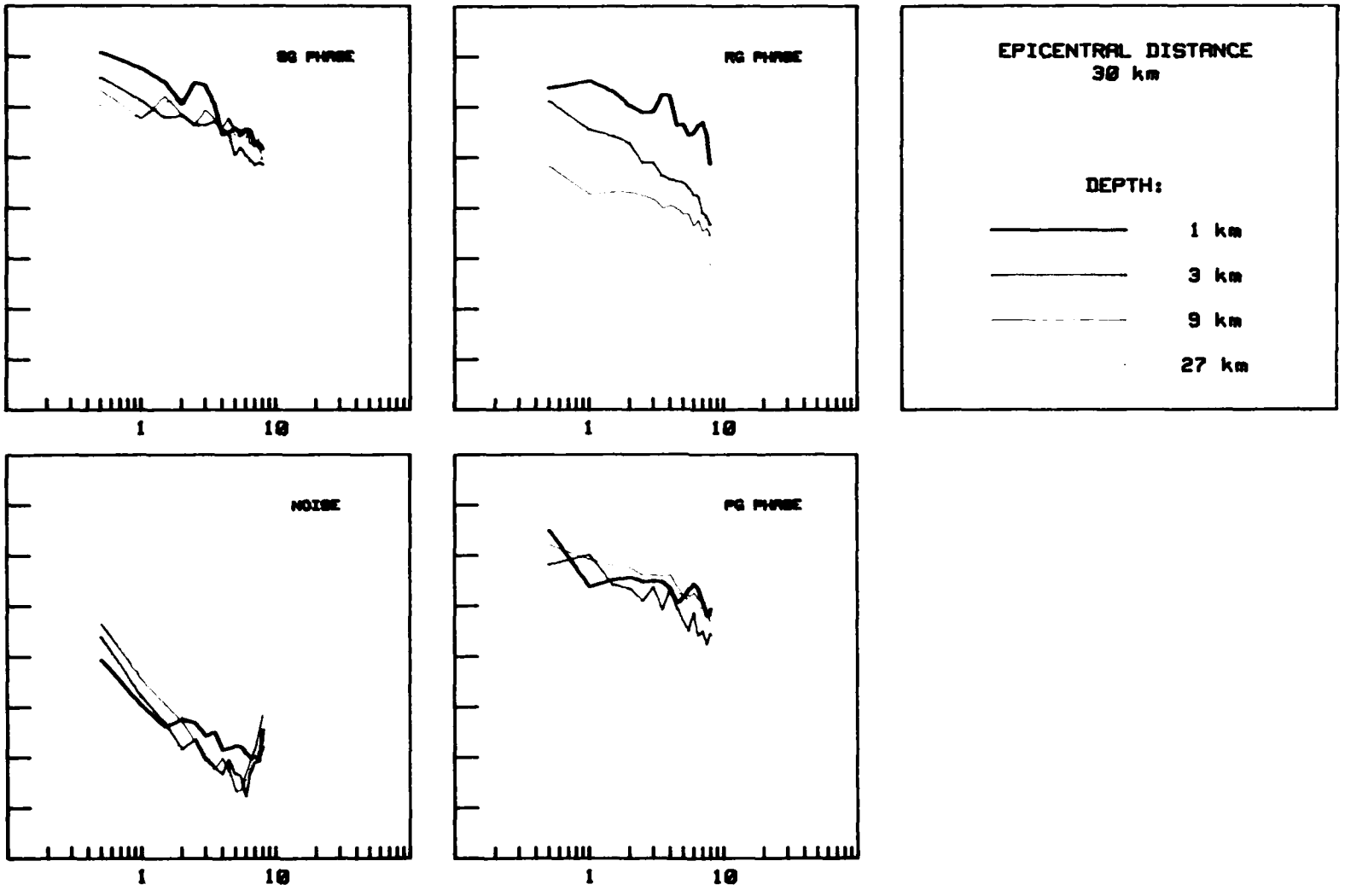

Fig. 2-c - SYNTHETIC DISPLACEMENT SPECTRA AT ONE EPICENTRAL DISTANCE FOR VARIOUS SOURCE DEPTHS

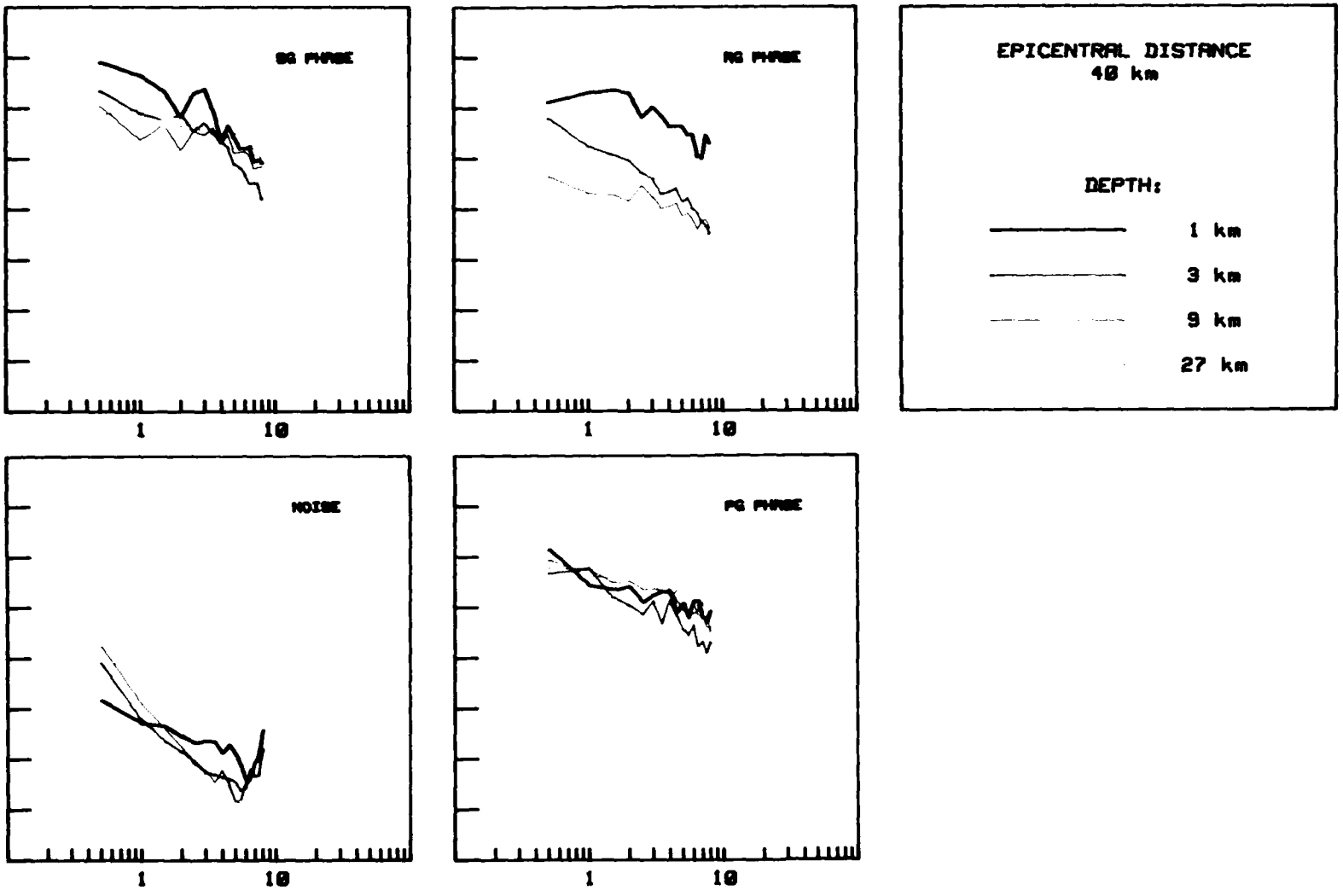

Fig. 2-d - SYNTHETIC DISPLACEMENT SPECTRA AT ONE EPICENTRAL DISTANCE FOR VARIOUS SOURCE DEPTHS

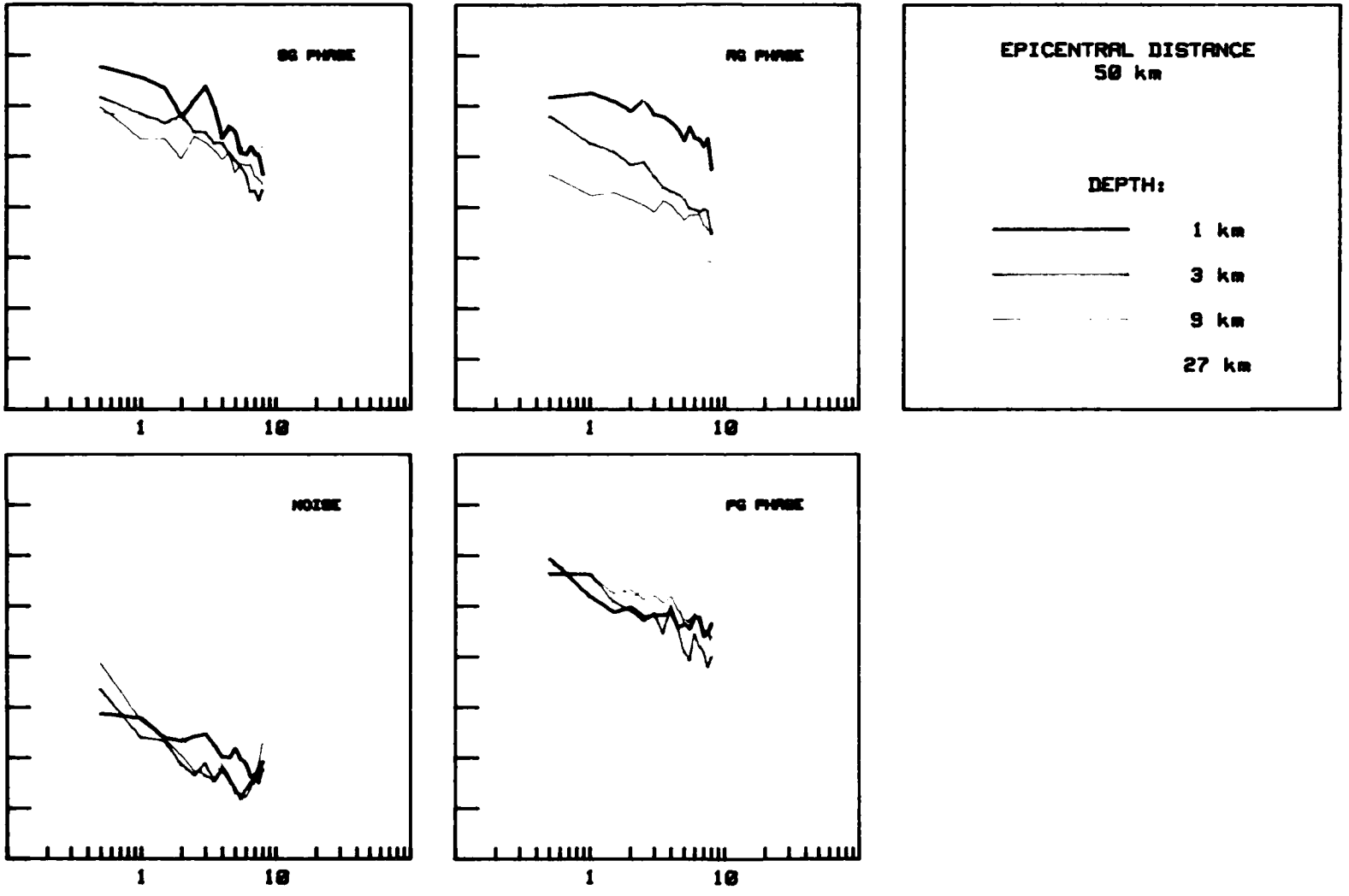

Fig. 2-e - SYNTHETIC DISPLACEMENT SPECTRA AT ONE EPICENTRAL DISTANCE FOR VARIOUS SOURCE DEPTHS

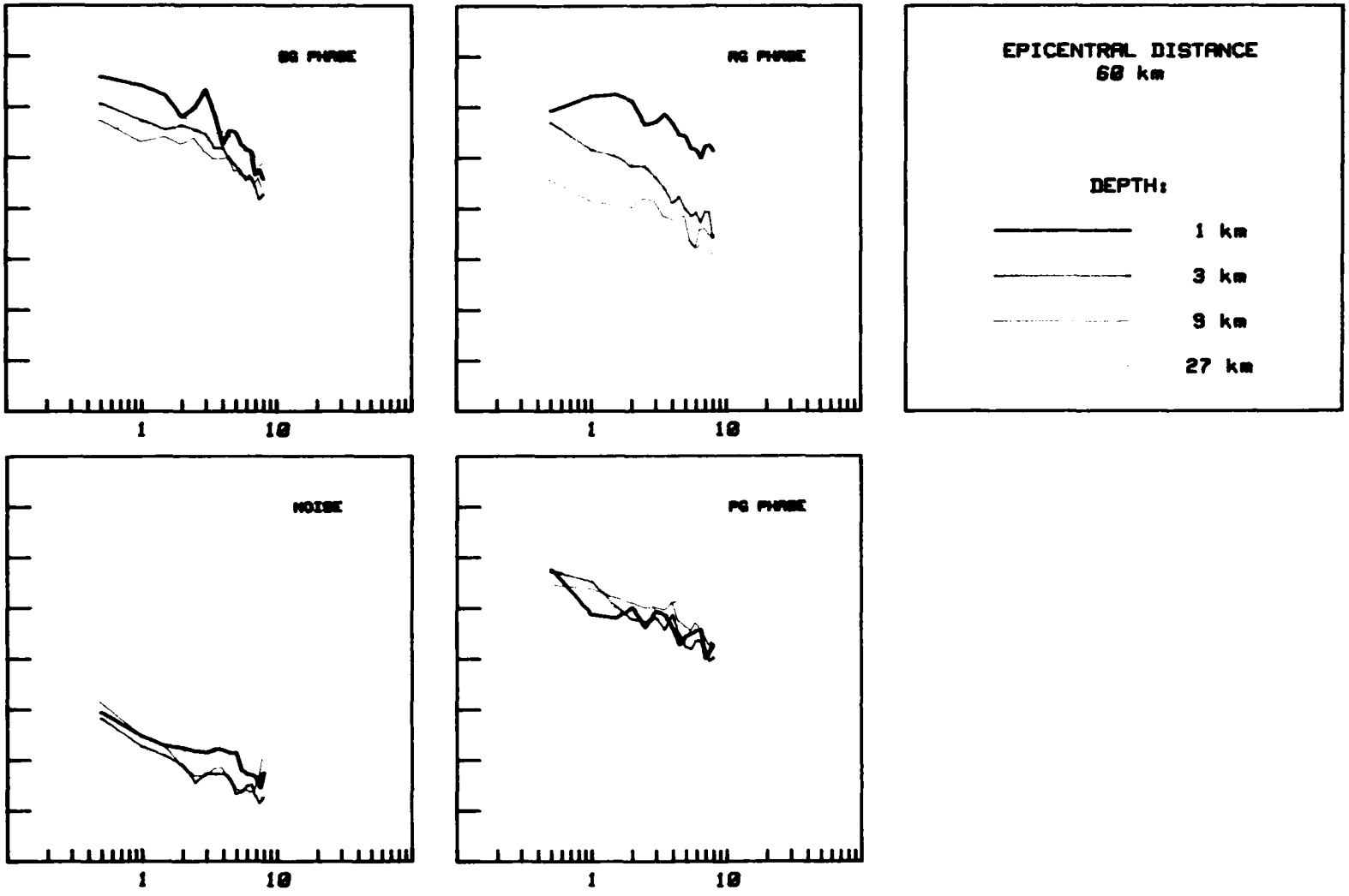

Fig. 2-f - SYNTHETIC DISPLACEMENT SPECTRA AT ONE EPICENTRAL DISTANCE FOR VARIOUS SOURCE DEPTHS

For Rg waves, geometrical attenuation is less effective but also depending on depth : 1,40 (1 km) increasing to 1,90 (3 km) and decreasing to 0,50 (12 km). At larger depths these waves are not excited and the geometrical attenuation coefficient has not more signification.

On the Fig. 3 are given the computed source spectra for each phase, at different depths and the corresponding Brune spectra obtained by least squares. Large differences between the original sources (Brune model) and the sources computed by inversion are observed especially in their low frequency part. They are not interpreted.

Nevertheless, if we represent (Fig. 4) amplitude ratio of these sources two by two (S/R, P/R, P/S) versus depth term we computed, we observe a sensible variation of these three numbers. (Amplitude is the low frequency mean value of the spectrum).

Although different points are still not be solved as the absence of flat frequency response of each computed source spectrum, we might expect to determine source depth ranges at local distances by a careful analysis of the relative importance of each phase.

Conclusion

By using synthetics computed for different source depths and for a distance range from 10 to 60 km, the source function has been inversed for different phases (Pg, Sg and Rg phases) defined by their group velocity; the propagation being caracterized by its geometrical attenuation only.

Besides a large dispersion of the results and the fact that it is not always possible retrieve the original source function used to compute the synthetics, it seems that the low frequency part of the displacement source spectra we obtained is strongly influenced by depth.

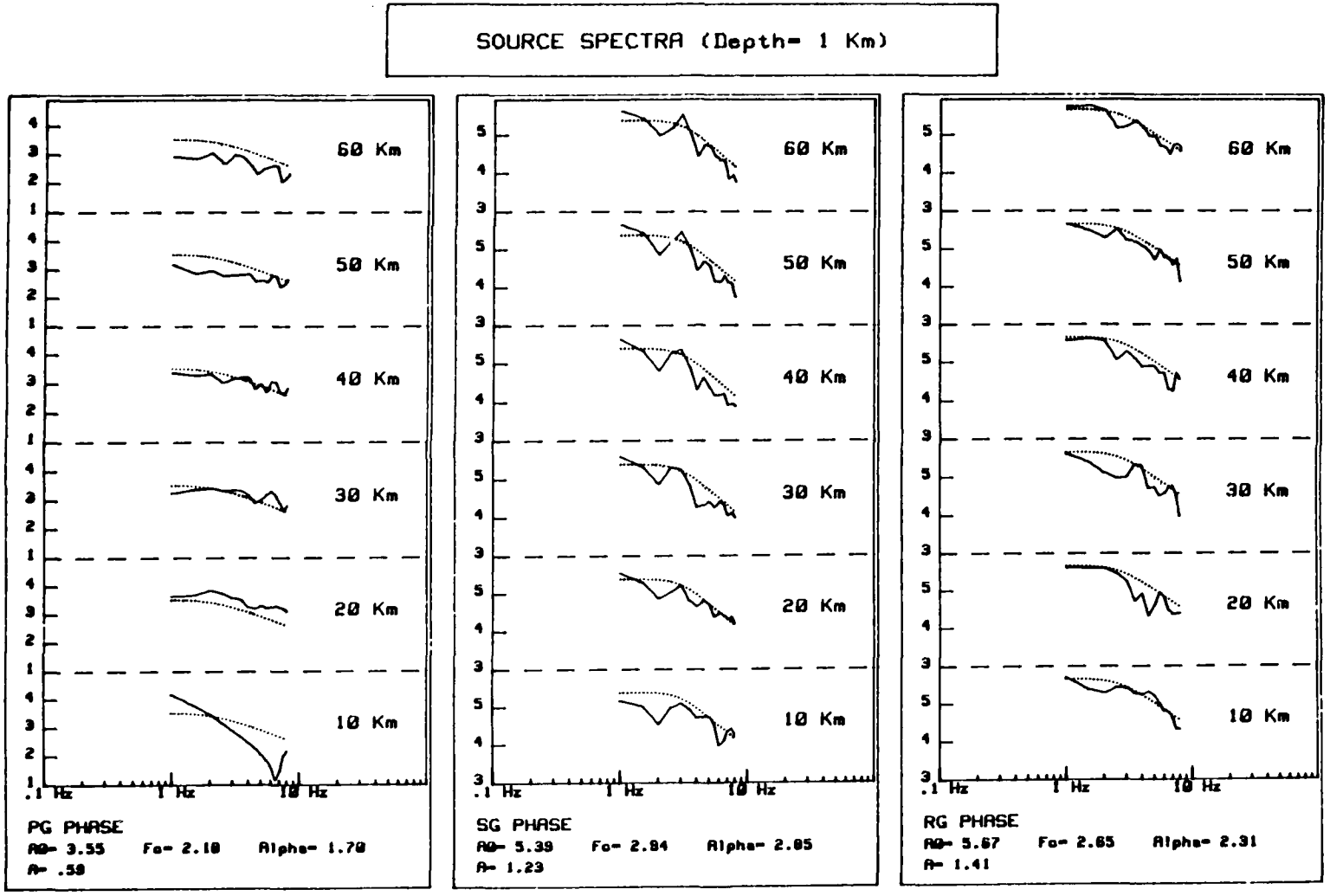

Fig. 3-a - CORRESPONDING TRUE SPECTRA IN DOTTED LINE (log-log scale) :
Ao : low frequency amplitude - fc : corner frequency - γ : HF slope - A : geometrical attenuation factor

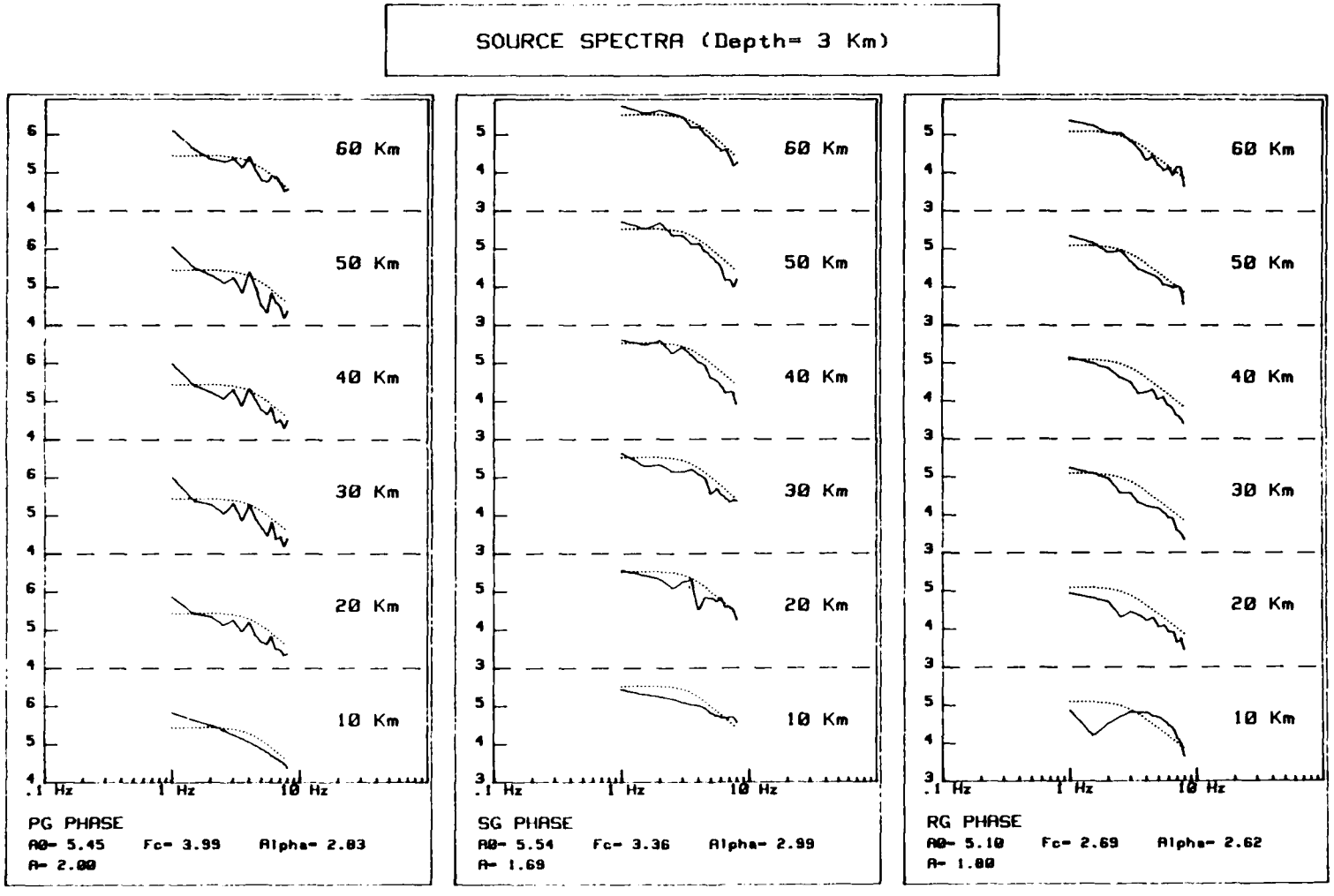

Fig. 3-b - CORRESPONDING BRUNE SPECTRA IN DOTTED LINE (log-log scale) :
Ao : low frequency amplitude - fc : corner frequency - ∝ : HF slope - A : geometrical attenuation factor

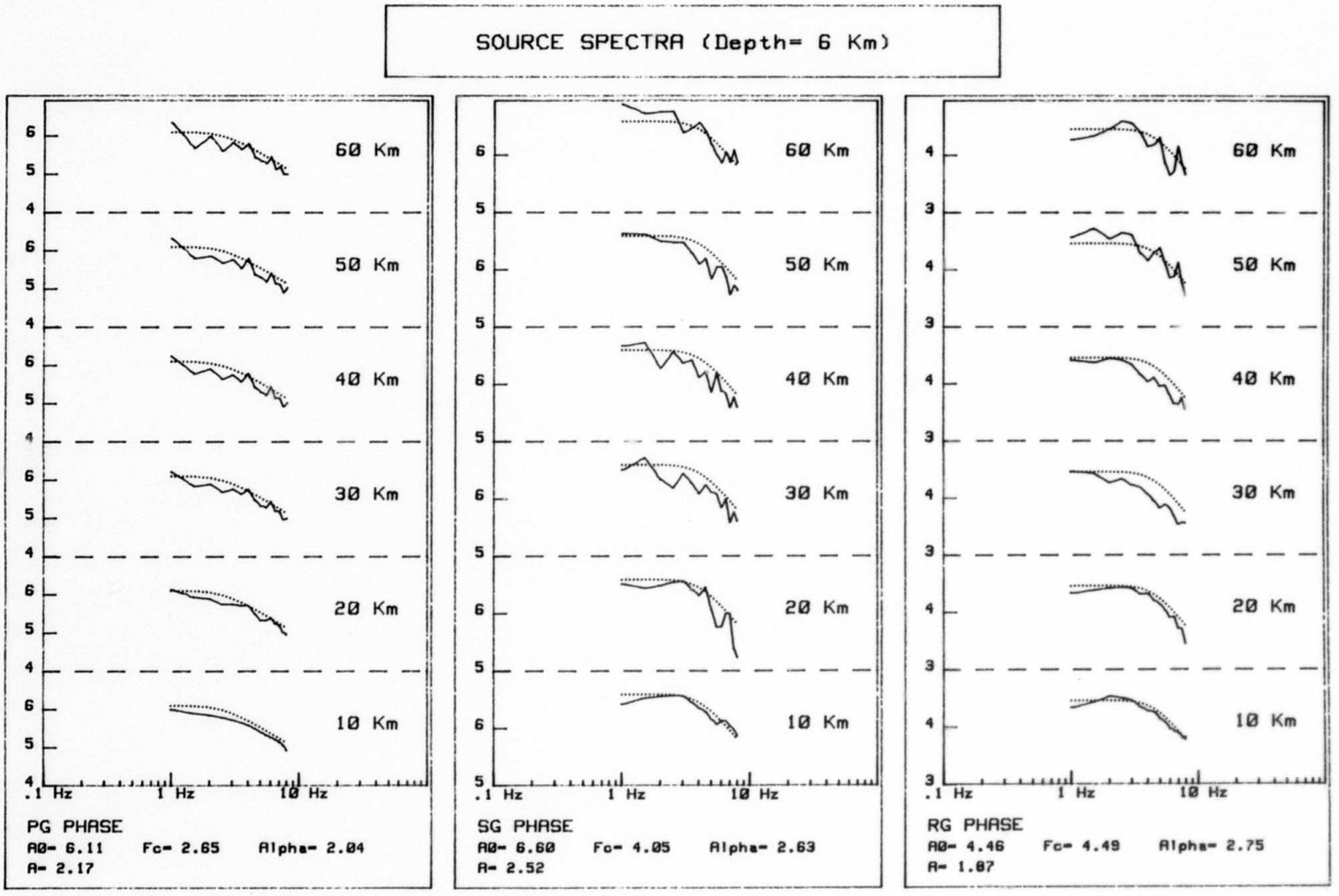

Fig. 3-c - CORRESPONDING BRUNE SPECTRA IN DOTTED LINE (log-log scale) :
Ao : low frequency amplitude - fc = corner frequency - α : HF slope - A : geometrical attenuation factor

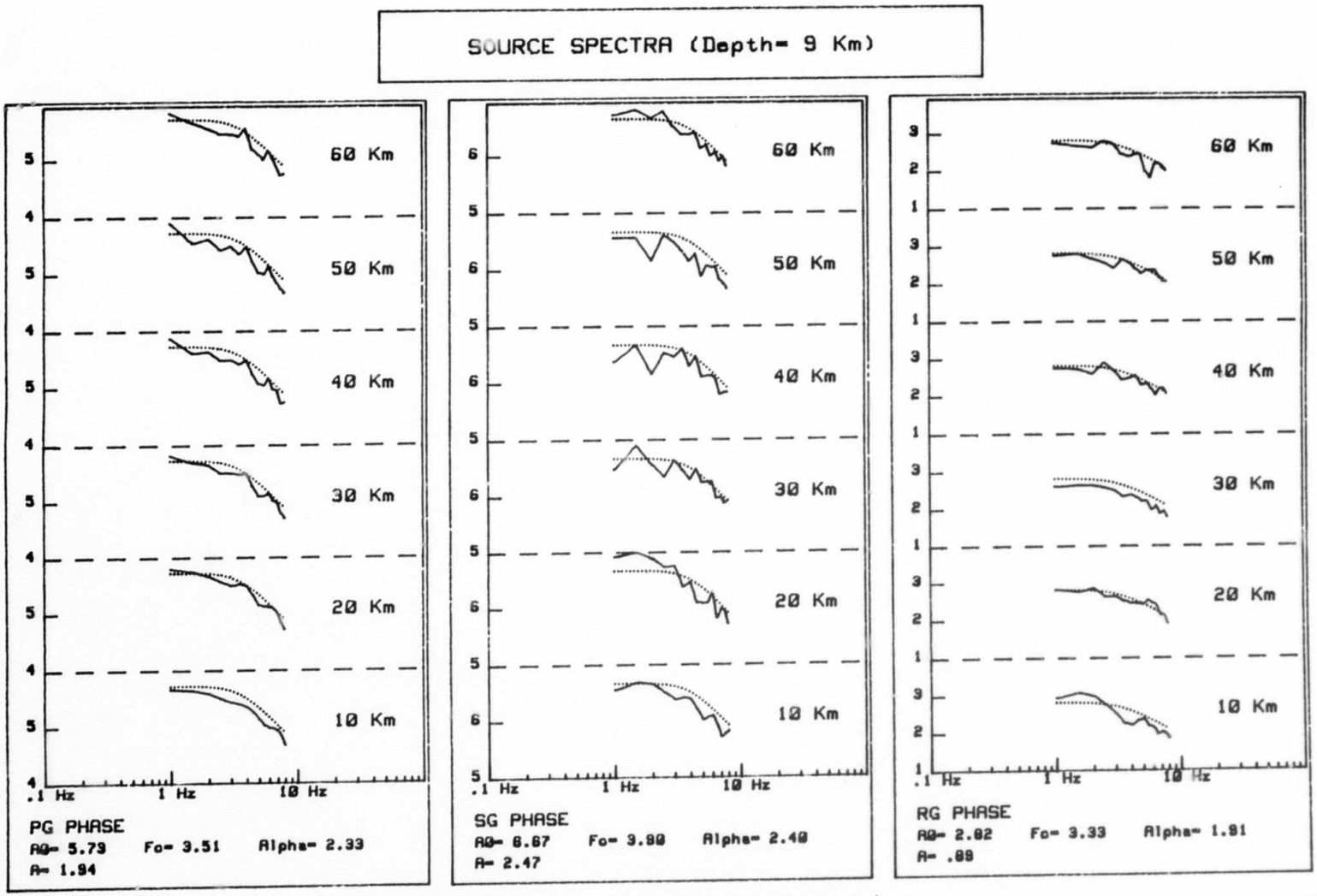

Fig. 3-d - CORRESPONDING BRUNE SPECTRA IN DOTTED LINE (log-log scale) :
Ao : low frequency amplitude - fc : corner frequency - γ : HF slope - A : geometrical attenuation factor

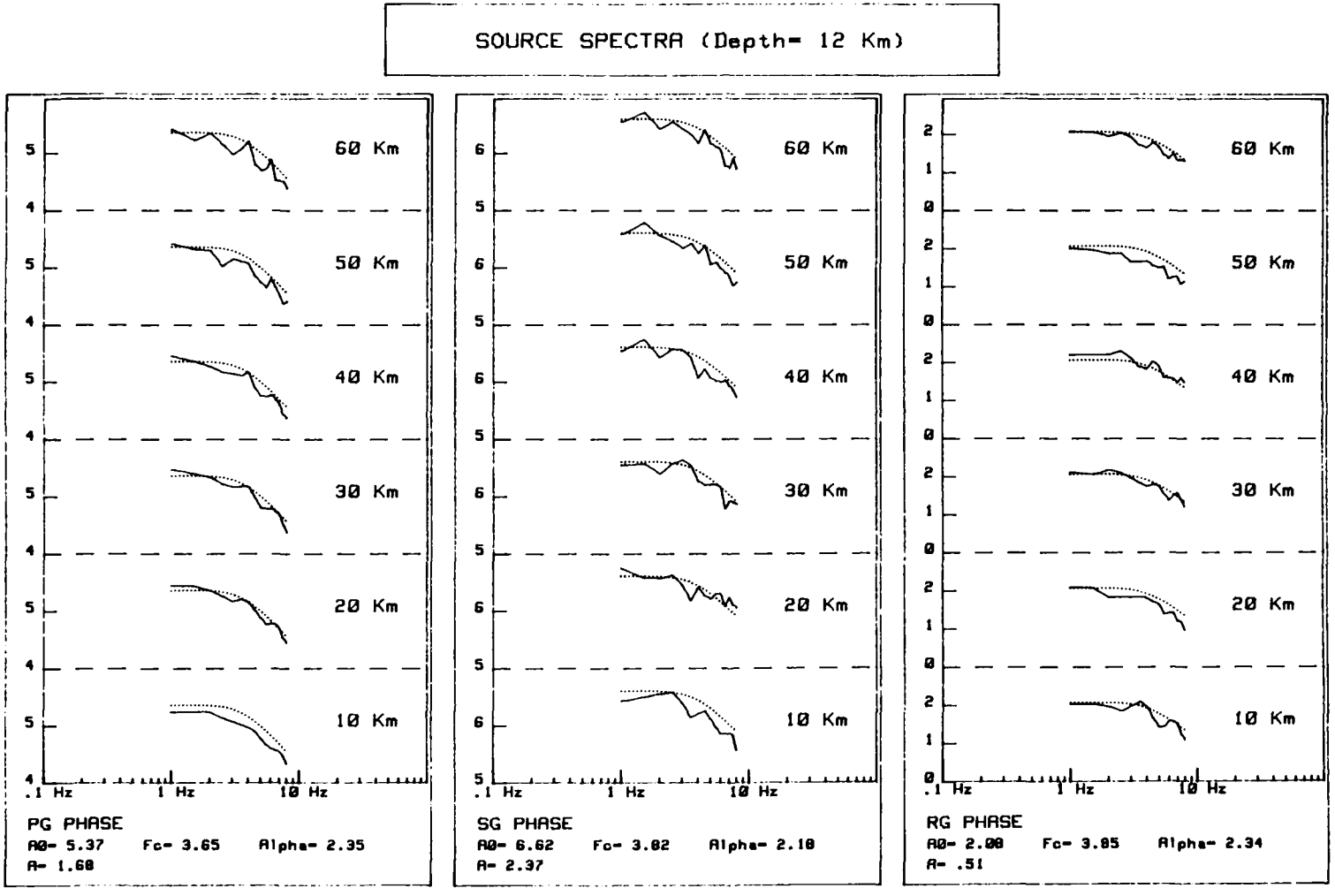

Fig. 3-e - CORRESPONDING BRUNE SPECTRA IN DOTTED LINE (log-log scale) :
Ao : low frequency amplitude - fc : corner frequency - ∧ : HF slope - A : geometrical attenuation factor

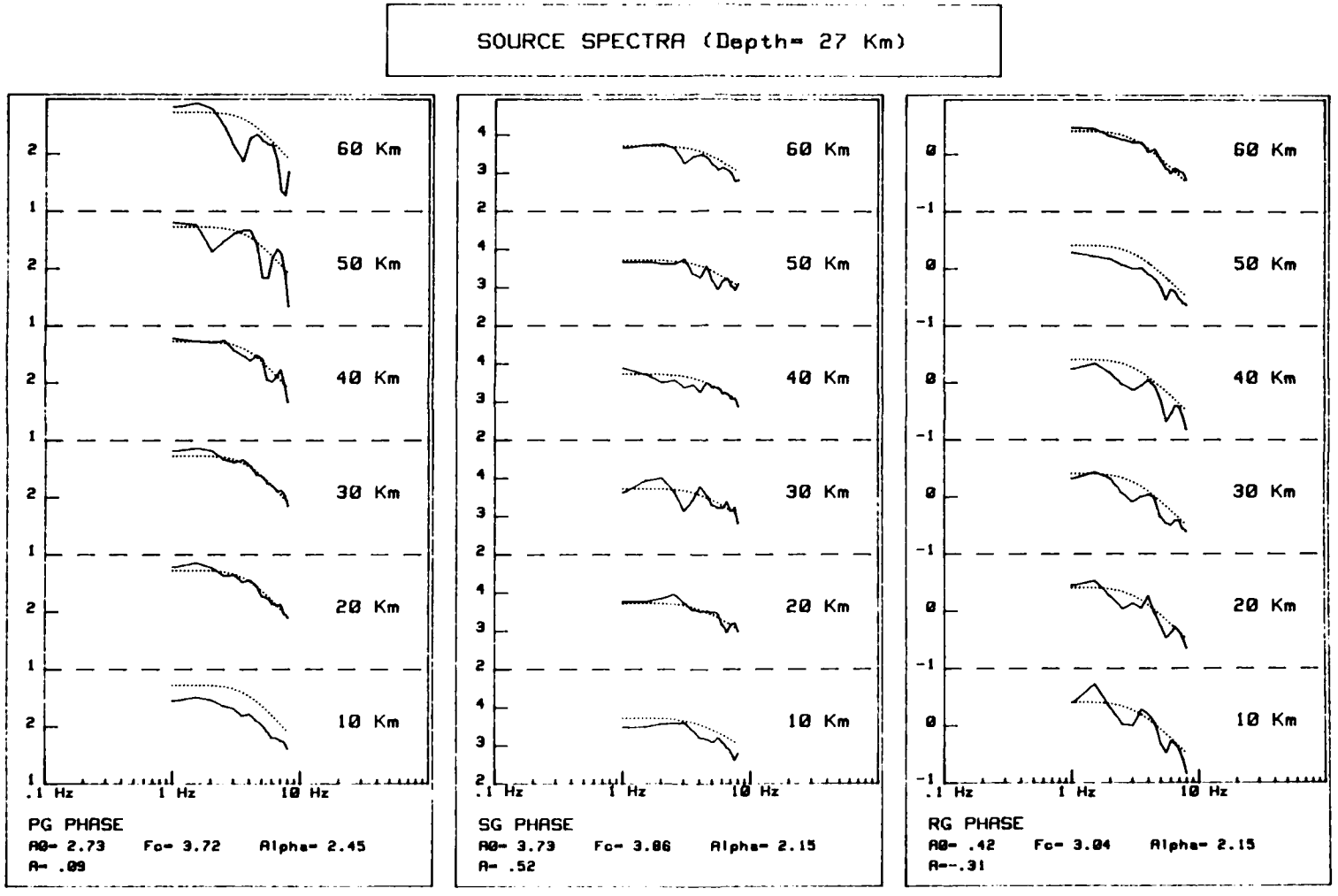

Fig. 3-f - CORRESPONDING BRUNE SPECTRA IN DOTTED LINE (log-log scale) :
Ao : low frequency amplitude - fc : corner frequency - 'n' : HF slope - A : geometrical attenuation factor

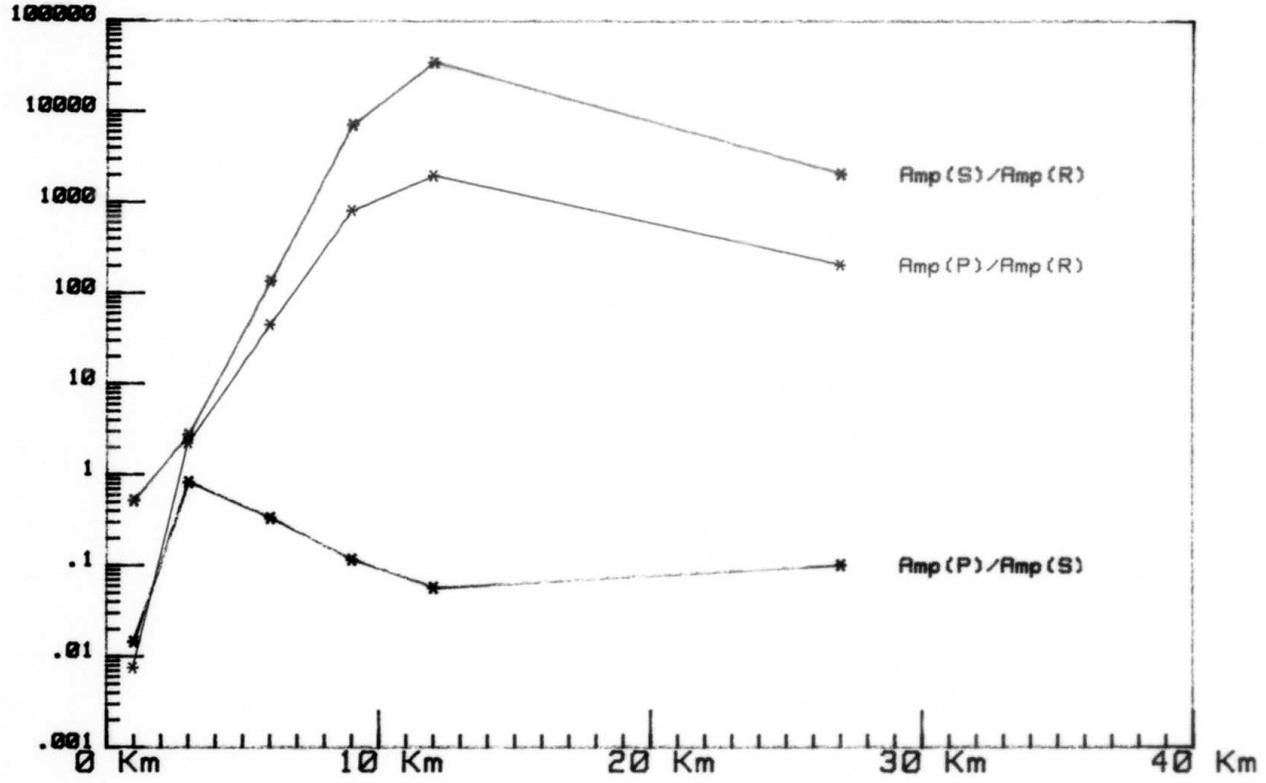

Fig. 4 - LOW FREQUENCY SPECTRAL RATIO VERSUS DEPTH

If that is confirmed, we might obtained information on the depth of a seismic event at least at local distances by using the ratio of Rg upon Pg low frequency spectra.

Nevertheless, it is necessary to verify that the curve we obtained is independant on the other source characteristics that is the source mechanism.

B - INVERSION METHOD ON Q(f) - Q TOMOGRAPHY ON FRANCE AREA

The studies we are carrying on to interprete the regional seismic phases in term of source energy have pointed out the main effect of anelastic attenuation.

After having studied the propagation of regional phases on a theoretical basis by synthetics, we have worked on the quantitative interpretation of the seismograms.

The data collected from the L. D. G. network have led, in a first step, to represent the anelastic attenuation by a mean quality factor depending on frequency.

This model has been confirmed by the coherency between empirical data and numerical simulation.

Consequently, it was possible to compute the source excitation function from each seismogram. The residual dispersion of source functions obtained by this way might be explained by a spatial heterogeneity of the quality factor in the France region.

This heterogeneity is associated to different geological units with proper quality factor and typical frequency dependancy.

As a result, we have used tomography techniques to evaluate the local quality factor.

A "back projection" application has pointed out a strong attenuation heterogeneity at 1 Hz which geographical distribution is strongly correlated with local geological characteristics.

These different results have led us to try to improve our seismic energy measurements from Lg waves analysis by taking into account the propagation anomalies.

For that purpose, it is necessary to draw a detailled map of the quality factor by an inversion technique at each frequency.
Such an operation needs a large number of data which are only available from natural sources.
The source energy at each frequency is becoming an extra-unknown for which the specific response of each station is to be added.

This study will allow an evaluation of the real resolution capacity in energy given by an homogeneous set of regional phases records.
The large amount of data and unknowns leads to use a technique of iterative reconstruction which needs not the resolution of large equation systems.
We have developped a program of local reconstruction (SIRT)*. This technique appeared to be well adapted to solve the very inhomogeneous spatial distribution between the source and each station.
We have introduced in the reconstruction algorithm a weighting function taking into account the possible redondancy of information due to the peculiar geographical distribution of natural seismicity. The weighting function applied for each seismic path, at each point is depending on path azimuth.

We have tested our program on synthetic models and on limited data sets and are just to proceed on a routine basis on a large amount of data recorded by the L. D. G. network and as we expect by other european digital networks (Switzerland, Italy).

* Simultaneous Iterative Reconstruction Technique

C - SOURCE STUDIES - DATA BASE

In 1986, we have achieved a regional seismic data base which includes the seismic data of 431 european earthquakes recorded on the french L. D. G. network (Fig. 1), during 1984 to 1986, with M_L magnitudes ranging from 2.4 to 5.7 (Fig. 2). All these quakes are within the crust but for most of them depth is not constrained.
The data base contains the seismic records (samples at 50 samples/sec) and the source spectra of each quakes computed on Lg_1 Lg_2 Lg_3 and Pg waves inversion techniques (see annual scientific report - 1985).

In order to select records with clear Lg waves, seismic signals are re-read from numerical mag-taps on paper records with a zero phase on Pg waves (Fig. 3 as an example).

Lg waves train is divided in three parts according to the group velocity :

Lg_1 waves $\quad 3,1\,km/s < V < 3,6\,km/s$

$2,6\,km/s < V < 3,1\,km/s$

$2,3\,km/s < V < 2,6\,km/s$

For each record, the amplitude spectrum is computed for each of the three Lg phases between 0,5 and 15 Hz. The seismic noise is also computed in front of each signal integration time in order to appreciate the usefull frequency band for the three Lg phases.

The whole set of spectra is the data base.

In order to test the data validity a first study on source spectra has been conducted by deconvolution of Lg spectra from the homogeneous attenuation model we obtain previously (Campillo and al., 1985).

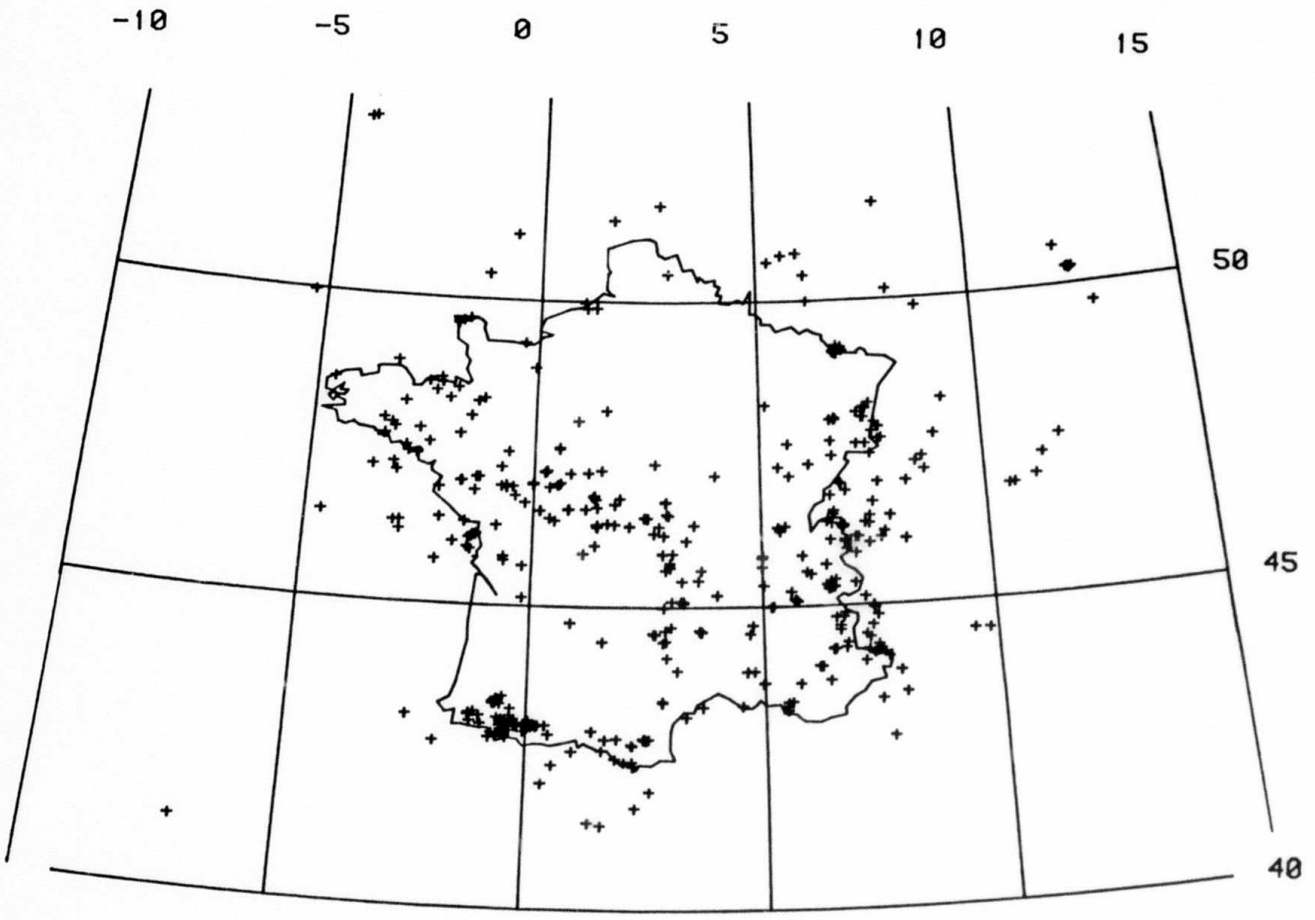

Fig. 1 - MAP OF THE 431 EARTHQUAKES USED IN THIS STUDY

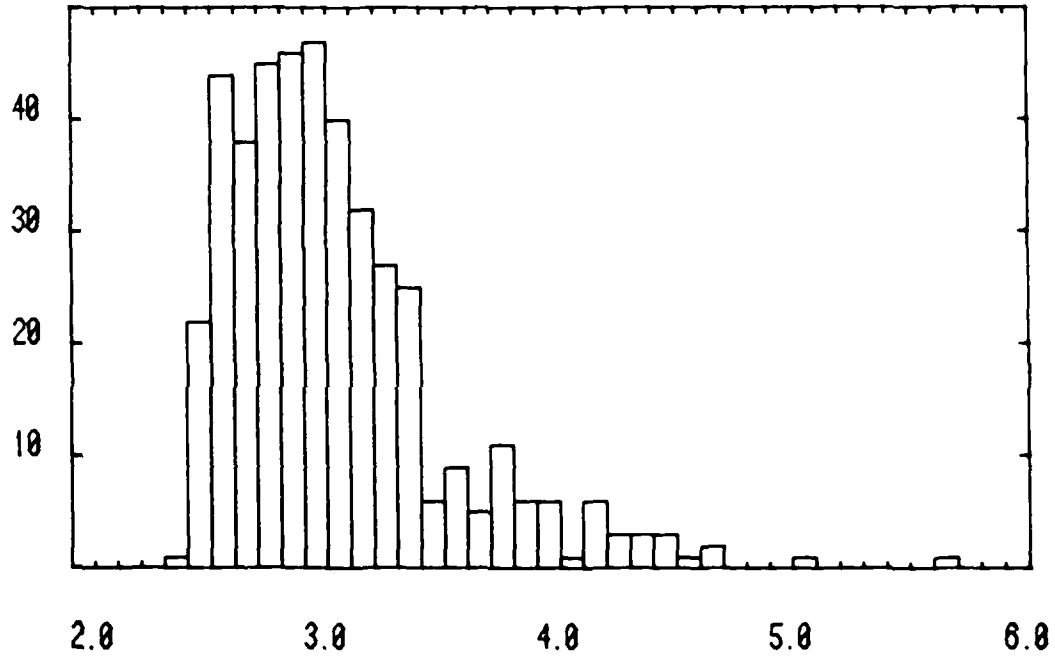

Fig.2 - NUMBER OF EARTHQUAKES VERSUS M_L MAGNITUDE HISTOGRAMS

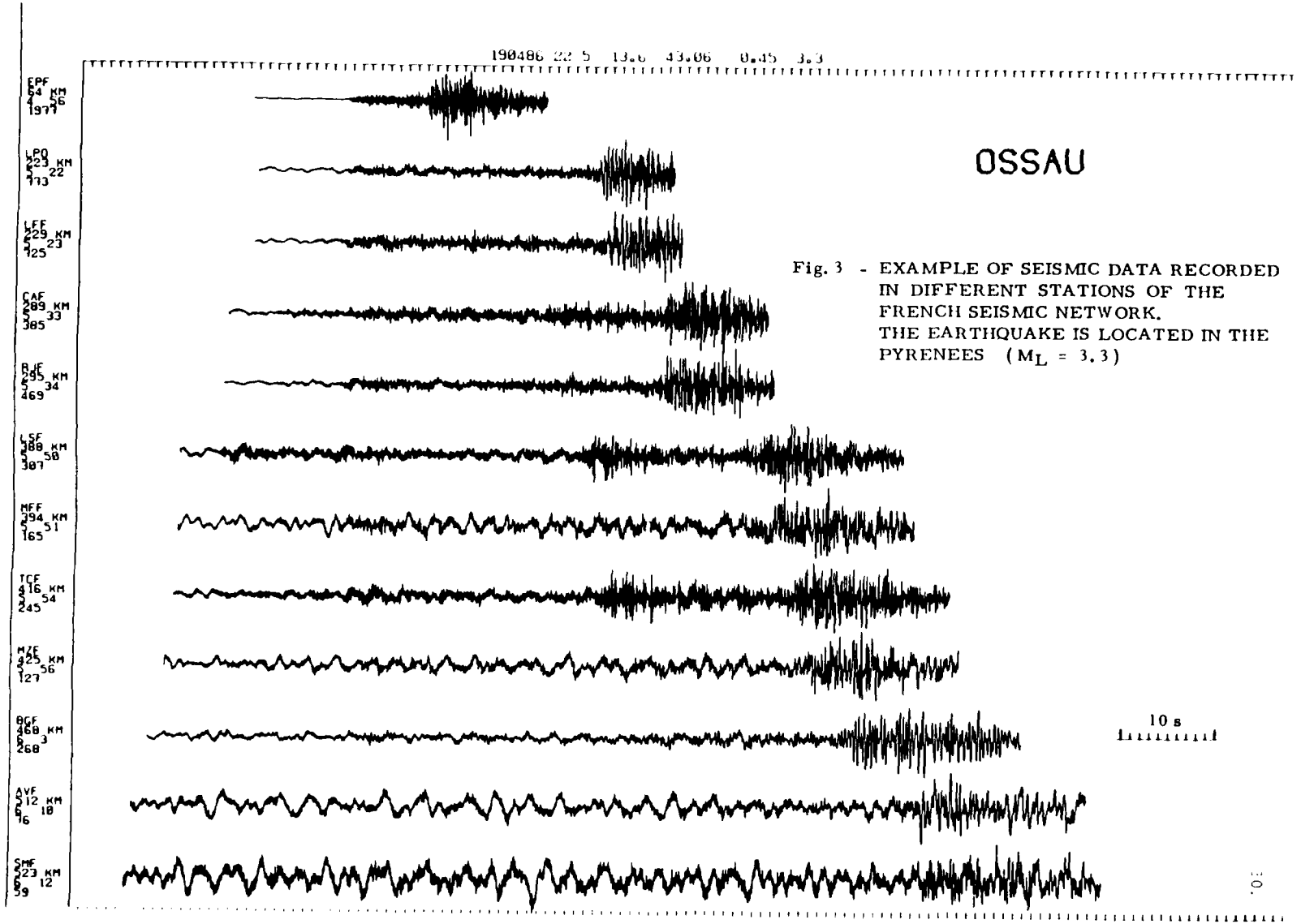

Fig. 3 - EXAMPLE OF SEISMIC DATA RECORDED IN DIFFERENT STATIONS OF THE FRENCH SEISMIC NETWORK. THE EARTHQUAKE IS LOCATED IN THE PYRENEES (M_L = 3.3)

For each quake, the source spectrum is obtained from each phase Lg_1 Lg_2 and Lg_3, and also for the combinde phases set (Fig. 4).

A large amount of such spectra computed in each station have a large discrepancy which might be reduced in a reasonable scale by the introduction of a Q tomography.

When the dispersion on deconvolved spectra is not too larger - which is true for 50 % of cases - their mean value leads to obtain the source amplitude at a distance of 1 km and consequently an estimation of the seismic moment computed on Lg waves.

The source expression is defined as a Brune source of the form :

$$s(\omega) = \frac{s(o)}{\sqrt{1 + (f/fc)^{2\alpha}}}$$

and the sources are computed by least squares to fit this amplitude spectrum.

For the different parts of the Lg spectrum the seismic moment M_o is systematically computed and the relationships between M_o and M_L local amplitude are built up (Fig. 6, 7, 8).
We obtain :

$$M_{o\,Lg_1} = 15,0 + 1,4\ M_L$$

$$M_{o\,Lg_2} = 15,5 + 1,3\ M_L$$

$$M_{o\,Lg_3} = 15,6 + 1,2\ M_L$$

For the whole set of Lg phase :

$$M_{Lg} = 15,1 + 1,4\ M_L$$

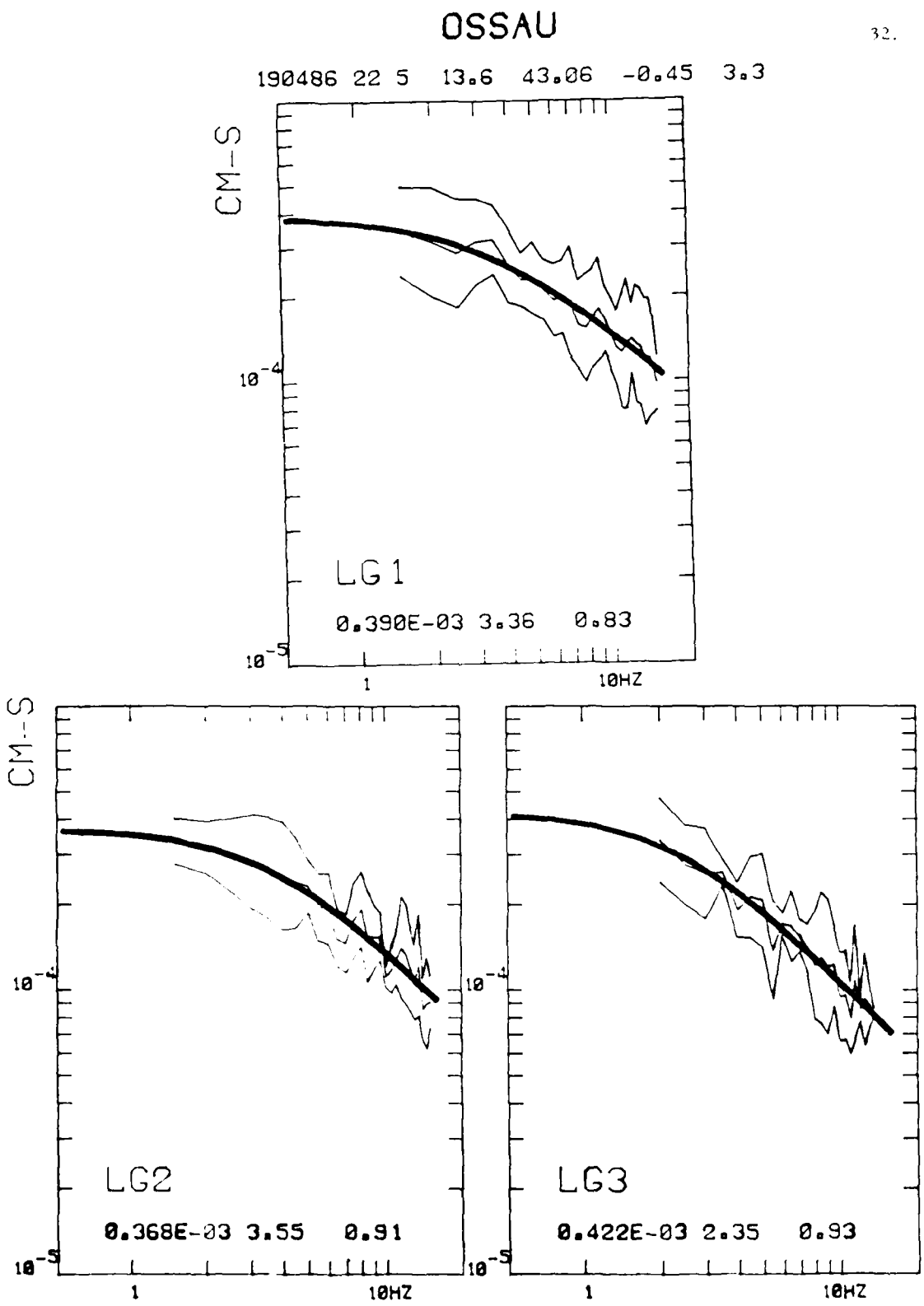

Fig. -a - SOURCE SPECTRA

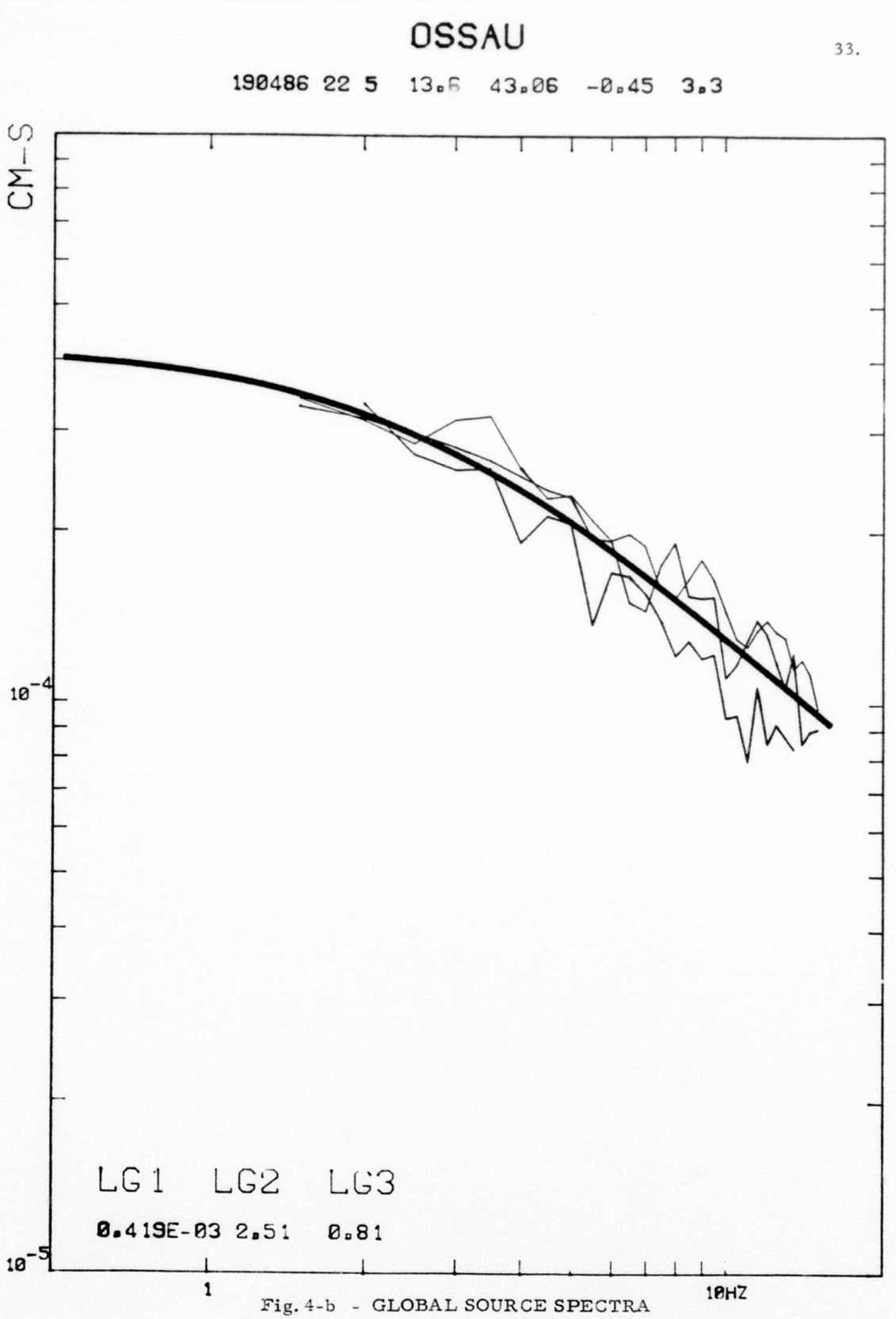

Fig. 4-b - GLOBAL SOURCE SPECTRA

As a result, the seismic moment variation versus magnitude is very similar for each part of the spectrum, according to the large discrepancy on both terms a_i and b_i from :

$$M_{Lg_i} = a_i + b_i M_L$$

This relationship $M_{Lg} = f(M_L)$ is compared with the relationships obtained in other parts of the world with close in epicentral seismic data

$M_o = 16,2 + 1,37\ M_L$ Japon

$M_o = 17,5 + 1,20\ M_L$ Californie

$M_o = 16,97 + 1,17\ M_L$ Yunam

For France area, the a term we computed is 1 or 2 units weaker than the previous ones, this might be interpreted as a source depth effect which was not be taken into account in our computation.

An attempt to regionalize quakes by peculiar $M_o = f(M_L)$ relationship did not lead to positive results. Q tomography might bring more accurate attenuation terms and so, allow some quakes regionalization if any.

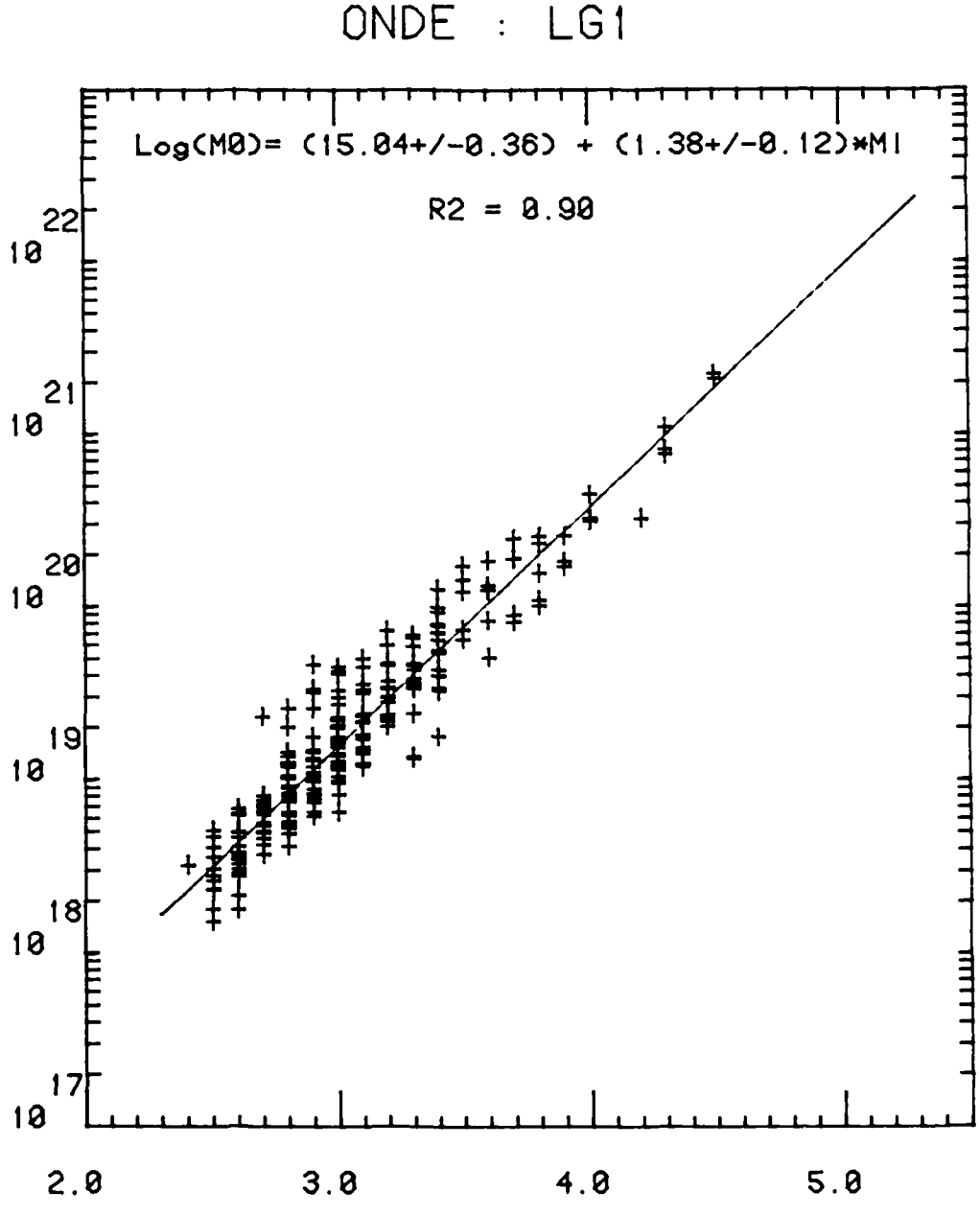

Fig. 5 - SEISMIC MOMENT M_o VERSUS M_L
(M_o in dyne-cm)

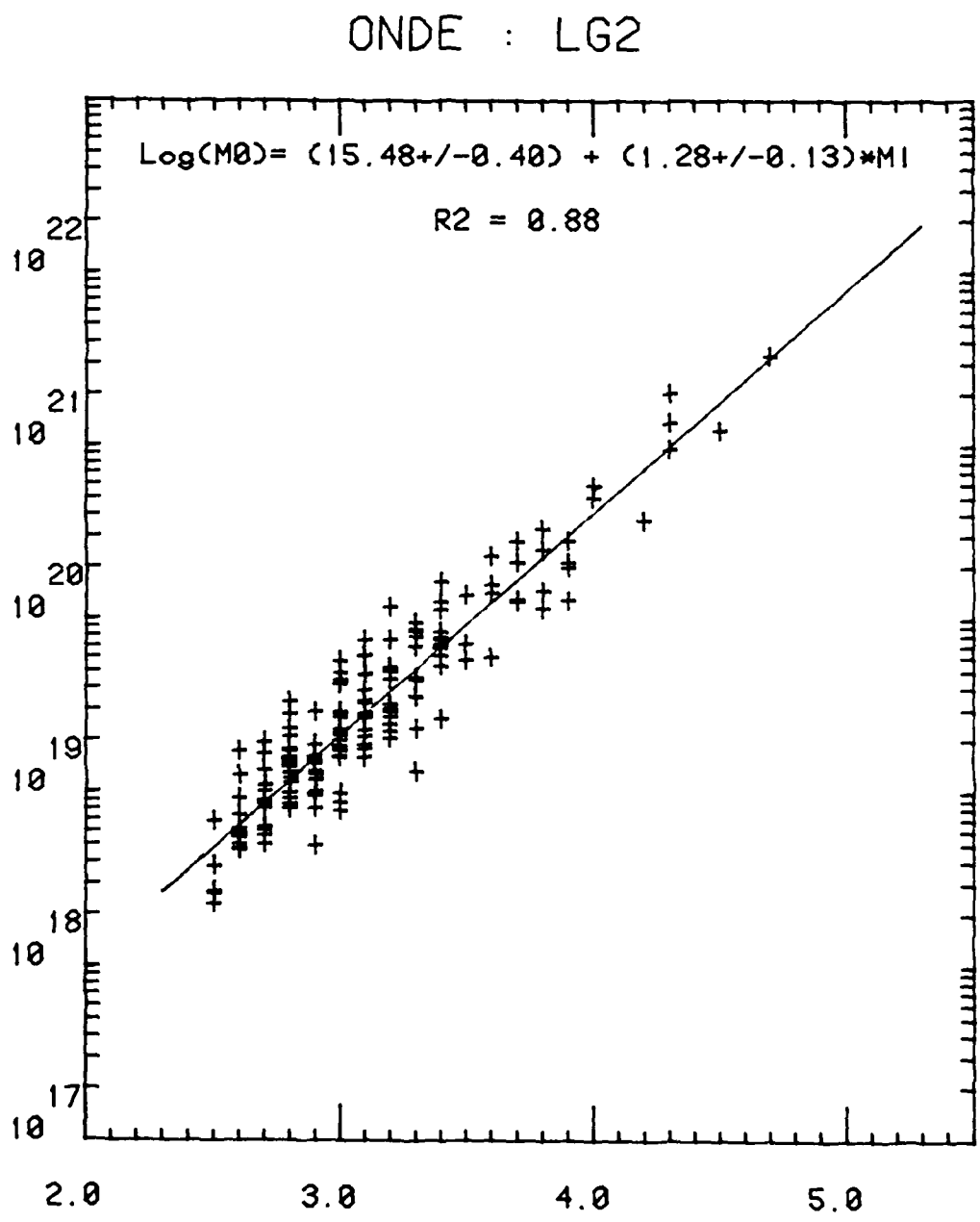

Fig. 6 - SEISMIC MOMENT M_o VERSUS M_L
(M_o in dyne-cm)

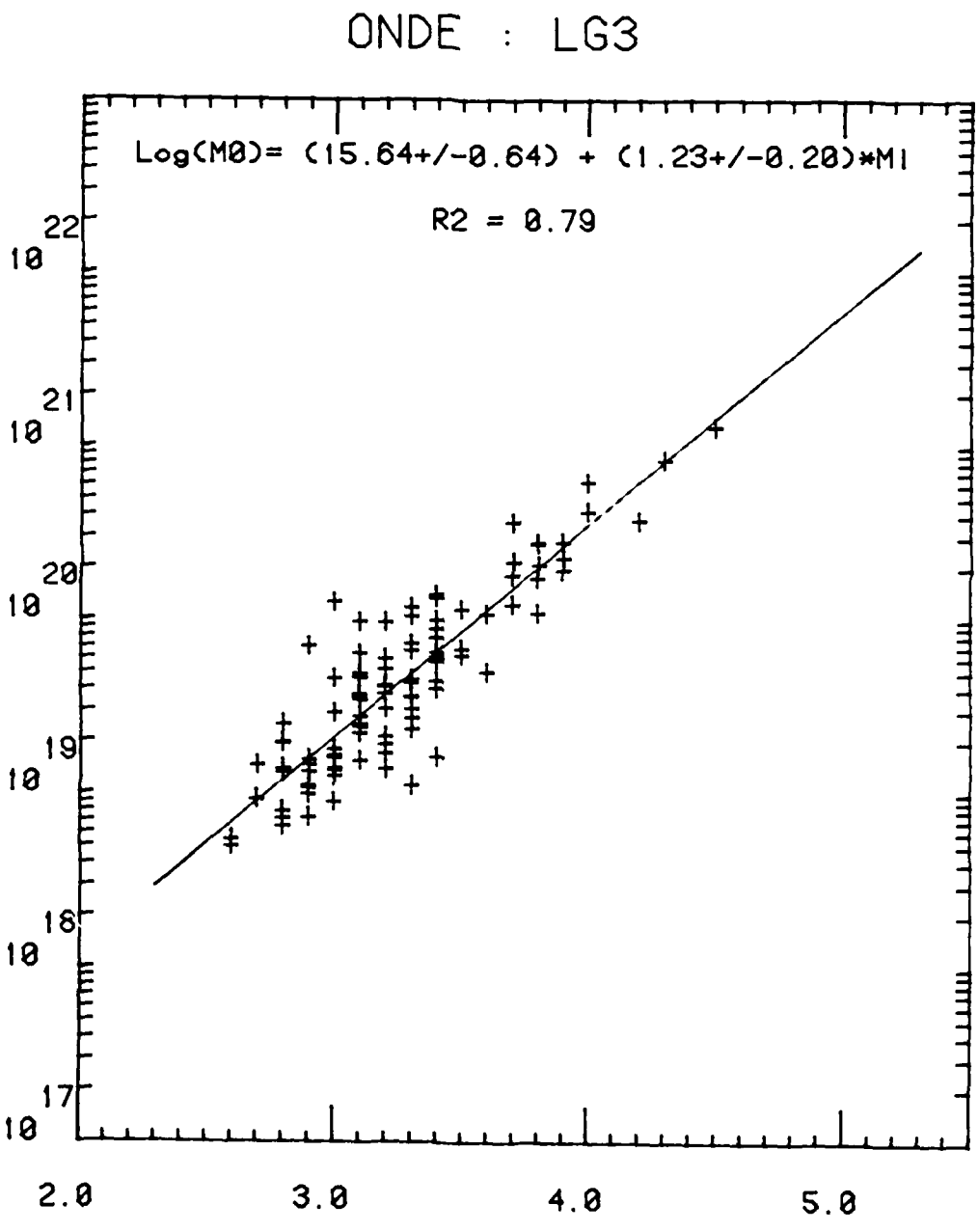

Fig. 7 - SEISMIC MOMENT M_o VERSUS M_L
(M_o in dyne-cm)

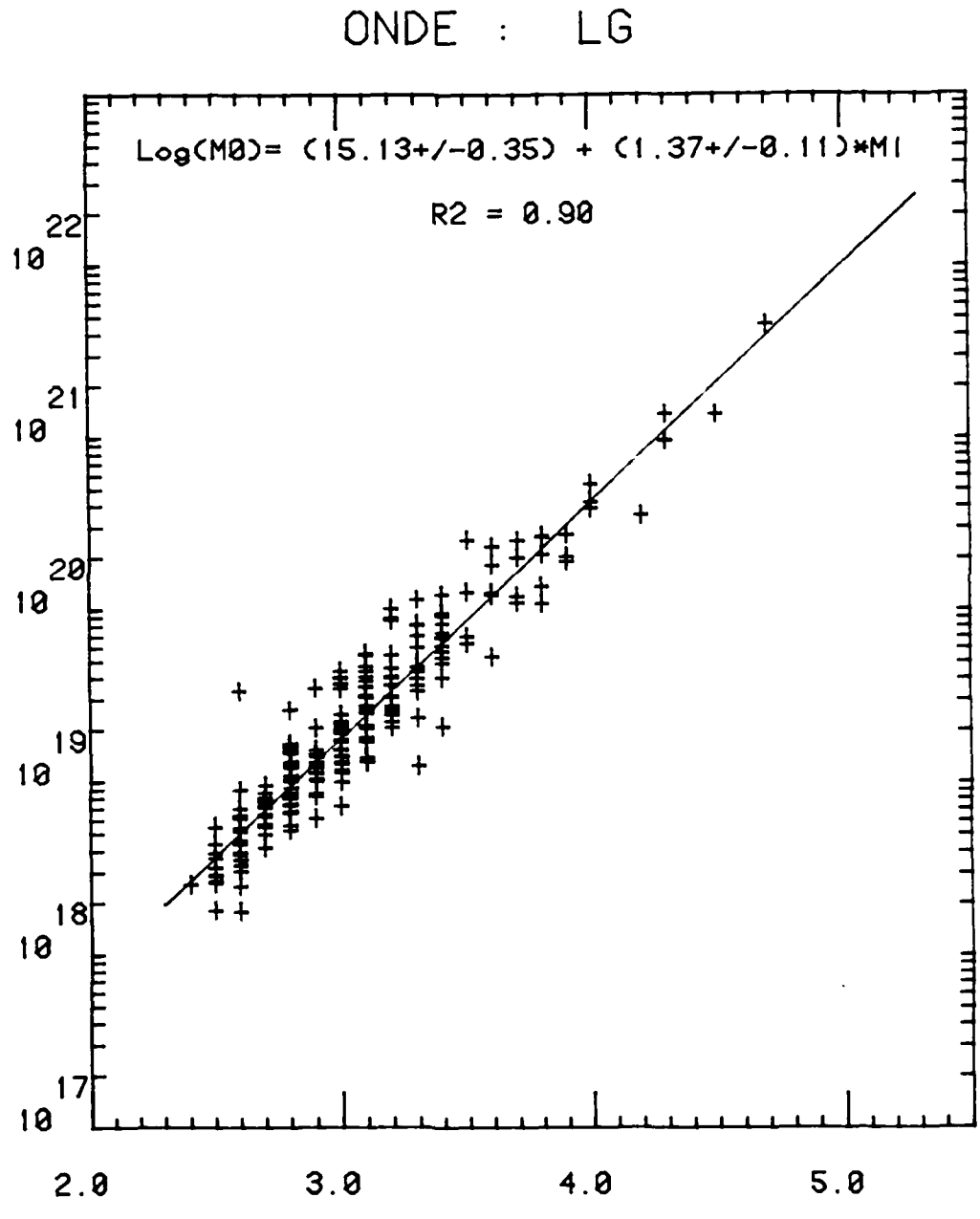

Fig. 8 - SEISMIC MOMENT M_o VERSUS M_L
(M_o in dyne-cm)

References

BOUCHON, M. (1981). A simple method to calculate Green's functions for elastic layered media, Bul. Seism. Soc. Am., 71, 959-971.

BOUCHON, M. (1982). The complete synthesis of seismic crustal phases at regional distances, J. Geophys. Res., 87, 1737-1741.

CAMPILLO, M., M. BOUCHON and B. MASSINON. (1984). Theoretical modeling study of the excitation, spectral characteristics and geometrical attenuation of regional seismic phases, Bul. Seism. Soc. Am., 74, 79-90.

CAMPILLO, M., J.L. PLANTET and M. BOUCHON. (1985). Frequency dependant attenuation in the crust beneath central France from Lg waves : Data analysis and numerical modeling, Bul. Seism. Soc. Am., 75, 1395-1441.

CRUSEM, R. (1986). Simulation de signaux sismiques et étude de sources nucléaires souterraines par inversion de moments, Ecole Centrale de Paris. Thesis.

MISTRAL, J. (1984). Analyse de la méthode de calcul des sismogrammes synthétiques par discrétisation du nombre d'ondes et applications. I.P.G./Strasbourg, Mémoire d'ingénieur.

BOATWRIGHT, J. (1978). Detailed special analysis of two small New York state earthquakes, Bul. Seism. Soc. Am., 68, 1117-1131.

BRUNE, J.N. (1970). Tectonic stress and the spectra of seismic shear waves from earthquakes, J. Geophys. Res., 75, 4997-5009.

D - PRESENTATIONS AT THE DARPA MEETING OF COLORADO SPRING - MAY 1986 -

AFGL / DARPA Seismic Research Symposium

U. S. Air Force Academy

Colorado Springs - 6-8 May 1986

Paper Tittle : Sources spectra determination for a recent seismic crisis in East of France (December 84-January 85)

Paper authors : B. Massinon - J.L. Plantet - Radiomana

Grant n° 85 0033

In the last annual report we have described a method (Campillo and al 1984) to extract from the Lg waves train the Q factor associated to the propagation region and the source spectrum.

We have applied these results for some quakes occuring in Remiremont (Vosges) in December 84/ January 85 and recorded on the seismic stations of the LDG network. The aim of this study was to evaluate the source amplitude spectrum for the main shock and some precursors and after shocks, and check if these results extracted from Lg waves in the far field were coherent with those obtained at short distance from the epicenter.

Seismic data :

Among the 28 SP seismic stations of the LDG network only 8 having recorded this crisis with a reasonable signal upon noise ratio have been selected. In the Figure 1 are represented the data recorded for the main shock (12/29/84 ; M_L = 4.8) and the stations versus epicenter repartition. All quakes are superficial, between 5 and 10 km depth. Seismic data are numerically recorded on magnetic tape with a sampling rate of the 50 samples / sec which allows to process signals spectra up to 15 Hz.

Figure 1

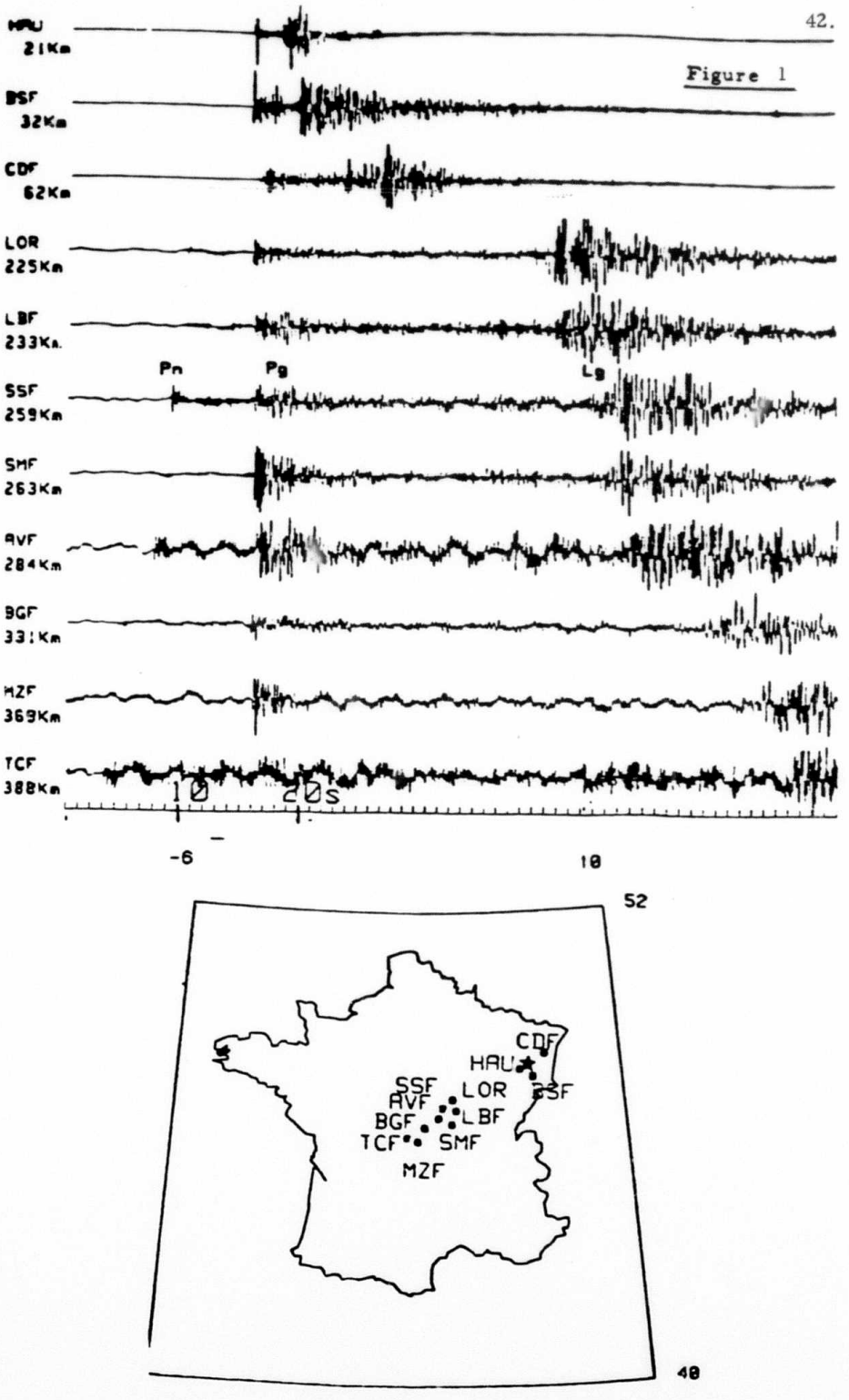

Seismic data and stations- epicenter configuration for the main shock (M_L = 4.8) Remiremont crisis

Results :

- After shock 01.02.85 $M_L = 4.0$:

This after shock is recorded at HAU station (Δ = 21 km) without saturation.

After deconvolution of the seismograph response, the amplitude spectrum of the Sg signal is computed.

It represents an amplitude spectrum of the source.

A source displacement model of the form :

$$\Omega(f) = \frac{\Omega(o)}{\sqrt{1 + \left(\frac{f}{fc}\right)^{2\alpha}}} \qquad \text{(Boatwright 1978)}$$

is computed by least squares to fit this amplitude spectrum (Fig. 2 a)

We find : corner frequency fc = 3.6 Hz

slope $\neq$ 1

The seismic moment Mo is also available by the following relation ship (Street and al 1975 ; Hermann and Kijko 1983)

$$Mo = \frac{4\pi \rho \beta^3 r_o \Omega(o)}{R_{\theta\phi}}$$

r_o = 1 km

$\Omega(o)$: displacement source spectrum at very low frequency

β : shear wave velocity = 3.5 km/s

ρ : density 2.2 g/cm^3

$R_{\theta\phi}$: coefficient taking into account both radiation pattern $\neq$ 1

We find $Mo = 2.8 \times 10^{20}$ dyne . cm

We also compute from Lg_1 , Lg_2 , Lg_3 waves trains recorded in the 8 stations situated at more than 200 km from the epicentral area, a mean amplitude source spectrum. For this computation we correct the Lg_1 , Lg_2, Lg_3 , spectra from :

- elastic and anelastic attenuation
- station response
- seismograph response

Figure 2

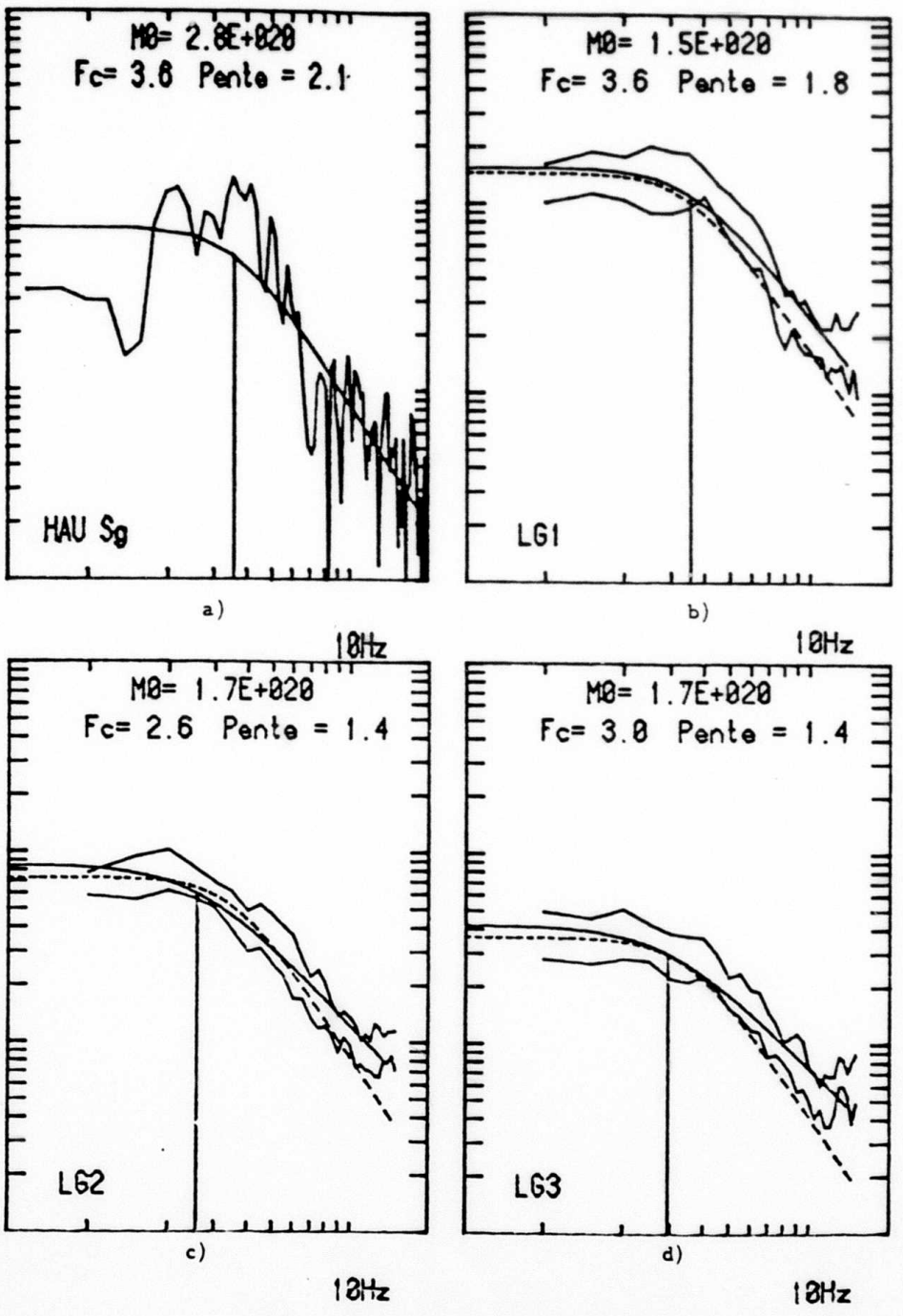

Remiremont crisis - Aftershock 010285 - M_L = 4.0

Figures 2 b , 2 c , 2 d represent an evaluation of the $\pm \sigma$ limits for the 8 source spectra and the mean amplitude source spectrum.
(continue line).
We also figure the source spectrum computed from HAU Sg waves (doted line) as a reference.
As a result , source spectra obtained with Lg waves in the far field are similar to the one obtained in the near field (HAU) namely. Lg_1 waves lead to a source spectrum which Ω (o), fc and slope are very comparable to those of HAU.
Seismic moments computed on the source spectra from Lg waves and the one extracted from Sg waves at HAU are of the same order.

- Main shock 12.29.84 $M_L = 4.8$

Source amplitude spectra on Lg_1 , Lg_2 , Lg_3 waves are computed by the same method described in the first case (After shock 01 02 85 $M_L = 4.0$).
For this main shock case no records are available at HAU.
Figure 3 represents the source spectra we obtain :
- $\pm \sigma$ amplitude spectra corresponding to all the 8 stations
- the source spectrum which fits the mean amplitude spectrum values.
- corner frequency fc , slope of the spectrum and seismic moments which are very similar .
- fault dimensions and stress drops computed for each of the three cases with, for the circular fault radius, two different formula proposed by Brune and Madariaga.

$$L = 0.37 \frac{\beta}{fc} \quad \text{(Brune)} \qquad L = 0.21 \frac{\beta}{fc} \quad \text{(Madariaga)}$$

and

$$\Delta\sigma = \frac{7}{16} \cdot \frac{Mo}{L^3}$$

Figure 3

	RAYON DE LA FAILLE	
	BRUNE	MADARIAGA
LG1	770m	430m
LG2	690m	390m
LG3	600m	330m

	CHUTE DE CONTRAINTE	
	BRUNE	MADARIAGA
LG1	20b	115b
LG2	40b	220b
LG3	85b	500b

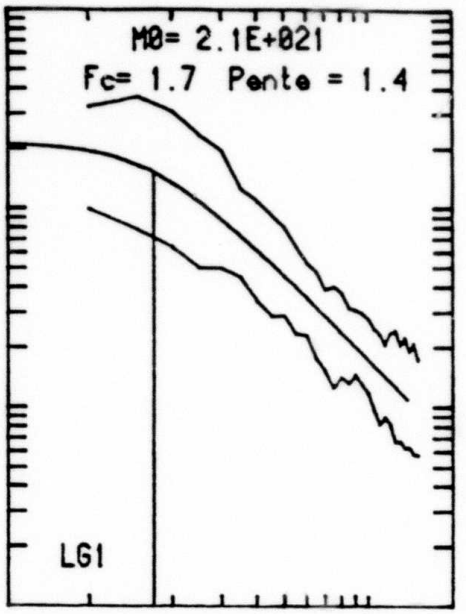

a)

10Hz

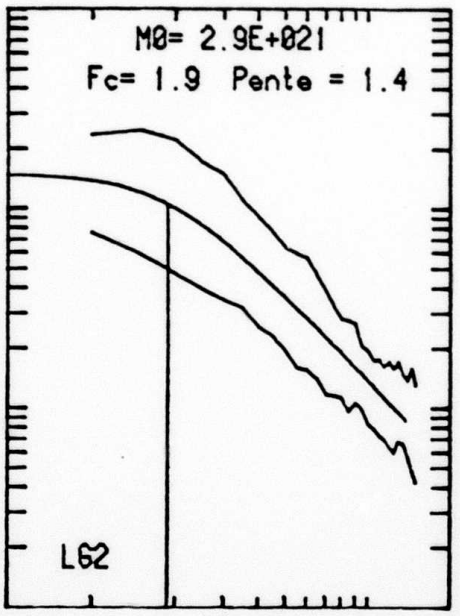

b)

10Hz

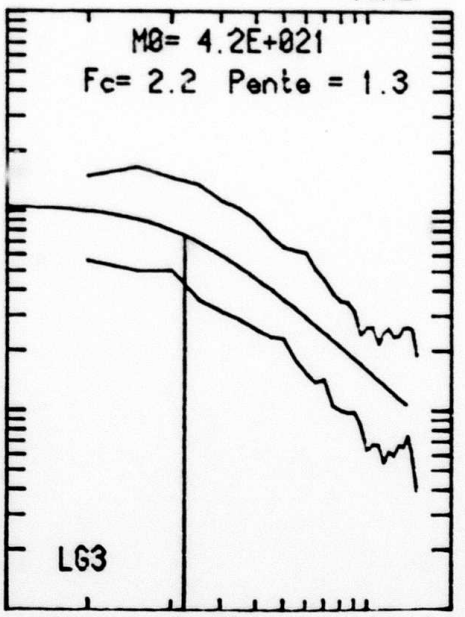

c)

10Hz

Remiremont crisis - main shock - 122984 - M_L=4.8

- Small foreshock 12.24.84 M_L = 3.0

This last example of source evaluation is given to figure out the limits of our far field method. This small foreshock is recorded by 8 stations among those which recorded the previous cases.

Figure 4 presents the source amplitude spectra obtained at HAU on Sg waves and on Lg_1 , Lg_2 , Lg_3 waves recorded on the 8 stations at 200 km and more from the epicenter. Computations and representations are identical as the ones of Figure 2 on the aftershock.

For this small foreshock the corner frequency is of the order of 7 to 9 Hz, to be compared to 3 , 6 Hz for the after shock (M_L = 4.0) and around 2 Hz for the main shock (M_L = 4.8).

The seismic moment is of the order of some 10^{19} dyne .cm.

But essentialy , the spectra definition particularly for Lg_3 waves and even Lg_2 is here rather poor and do not guarantee a reasonable fiability on the results.

Conclusion :

This attempt to evaluate the source amplitude spectrum of the earthquake by processing the Lg waves train recorded at large distances seems to be reliable as shown on the Remiremont seismic crisis.

It is necessary to apply this method on more different cases but we notice already that as long as the Lg waves are well defined, they bring information from the source which lead to approach its main parameters.

Figure 4

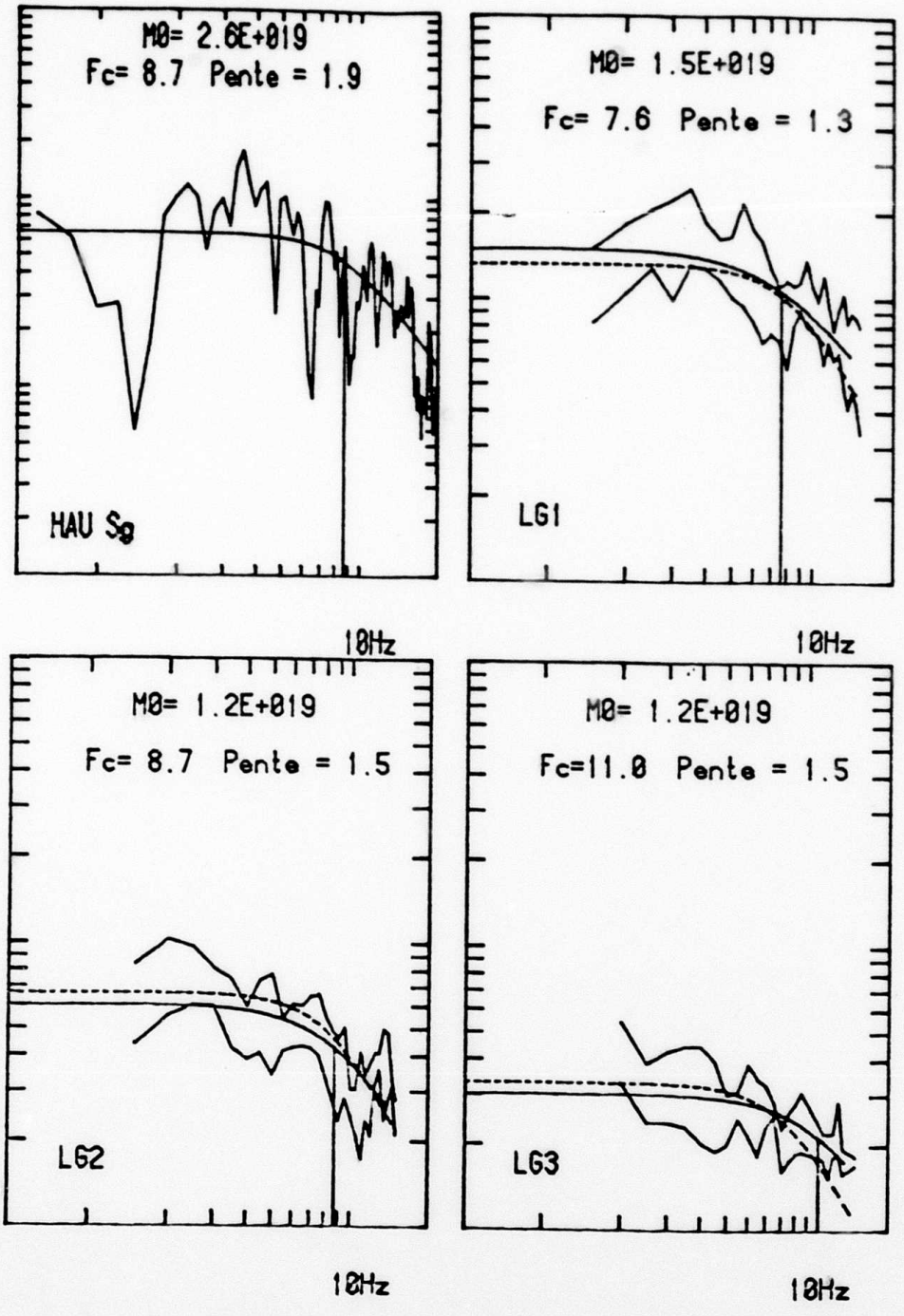

Remiremont crisis - Foreshock 12 24 84 - M_L = 3.0

AFGL / DARPA Seismic Research Symposium

U. S. Air Force Academy

Colorado Springs- 6-8 May 1986

Paper Tittle : Propagation of Lg waves through a laterally heterogeneous crust

Paper authors : M. Bouchon and M. Campillo - Radiomana

Grant n° 85 0033

Introduction

The method used in that study is derived from the discret waves numbers method. It has been used to characterize the effects of different large scale heterogeneities on the Lg waves propagation.

Two types of effect have been studied.
First, the effects due to Moho irregularities. The Lg waves train is a superposition of reflected S waves trapped within the crust. Consequently any variation of the Moho depth might affect the waves guide quality and leads to some apparent strong attenuation zone for Lg waves.
Second, we look at the effects of sedimentary basins on the Lg waves propagation path.

The study is limited to the SH in two dimensions. Irregularities dimensions are selected to fit the situations met in central part of France for which general attenuation features have been studied (Campillo , Plantet and Bouchon 1985).

I Variation of the Moho depth

The crust model is given in Figure 1. Computations have been made for seismic sources at 10 km depth, located at 0, 50, 100, 150 and 200 km from the Moho irregularity.

Figure 2 shows maximum amplitude variations for Lg waves versus distance, for a planar crust mode (thick solid line) and for a crust model with irregularity at these previous distances.

In the irregularity vicinities, steepen reflectors bring strong amplitude variations.

On the contrary, at larger distances, no important and systematic differences are seen between a Moho without or with irregularity.

This points out that any Moho ascent should commonly bring limited attenuation effects on Lg waves.

II Sedimentary basin

We look now at the influence of a thicken sedimentary layer or a sedimentary basin as described in Figure 3 on Lg waves at the same distances from the irregularity(as describe in Figure 1) seismic sources are always at 10 km depth.

The synthetic seismograms are presented in Figure 4 for various distances from 0 to 290 km, every 10 km, for both a planar crust (upper seismograms) and a thicken sedimentary layer at the top of the crust (lower seismograms).

Clearly seen is the formation of a Love wave in the case of a sedimentary basin. As superficial layers are propagation structures which strongly affect Love waves, the converted Lg waves to Love waves energy will be rapidly dissipated.

Within the sedimentary basin itself, classical amplification phenomena might happen.

These two rough synthetic examples suggest to verify their conclusions for some real cases.

III Regional distribution of apparent attenuation in the center of France

The set of seismic data which leads to the evaluation of the quality factor

$$Q = Q_o f$$

for the center of France in a recent study is used to build up an image of the Q factor spatial distribution.
The method we use is the ART (Algebric Reconstruction Technics).

The set of used propagation paths for the 1 Hz reconstruction (that is to say : Q_o) is presented in Figure 5.
Each point of the image is taking into account the paths within a distance of 50 km.
In order to apply some confidence criterium on the quality of the Q evaluation we define a confidence index :

$$i_c = n_{source} \times \sum l_r$$

where : n_{source} is the number of sources which spectra are different, used for the Q measurement.

l_r is the ray path lenth within the influence circle (of 50 km radius at the most) divided by the influence radius.

A map of these factors i_c is shown in Figure 6. All the represented points fit the length of ray test.
All the blue zones correspond to a high confidence index; red zones might include systematic bias.

Figure 7 represents a rather simple regional distribution. If one just keeps within high confidence limits, three main regions are defined.
- Limagne Basin, Forez, Saone valley : weak figure for Q (between 180 and 240)
- Limousin : Q between 200 and 260
- South parisian basin, Berry, Poitou, North of Massif Central Q between 300 and 440
- At 1 Hz the mean value for Q on the whole studied zone is 290 as mentionned in a last study.

Conclusion

These results pointed out the importance of graben zones for L g waves propagation. Nevertheless, at this stage of the study we do not possess any separation tool between two types of phenomena which could create attenuation :

- small scale diffraction (or scattering)
- large scale geometrical effect.

A study of frequency dependancy for Q should help in the interpretation of our data.

On the other hand, developments of numerical simulation methods encourage us to investigate more complex zones in order to interprete the quasi-extinction phenomena of Lg waves we have observed along peculiar paths.

Figure 1 : crust model with Moho irregularity - the star is the seismic source - seismograms are built at various distances.

Figure 2 : maximum amplitudes of Lg waves versus distance (2D).

Figure 3 : crust model with a sedimentary basin

Figure 4 : synthetics obtained with a planar crust model (high) and with a sedimentary irregularity (low)

Figure 5 : Rays paths used to build up a map of Q_c factor for France

Figure 6 : Map of confidence index

Figure 7 : Map of France (Center) for Q factor at 1 Hz

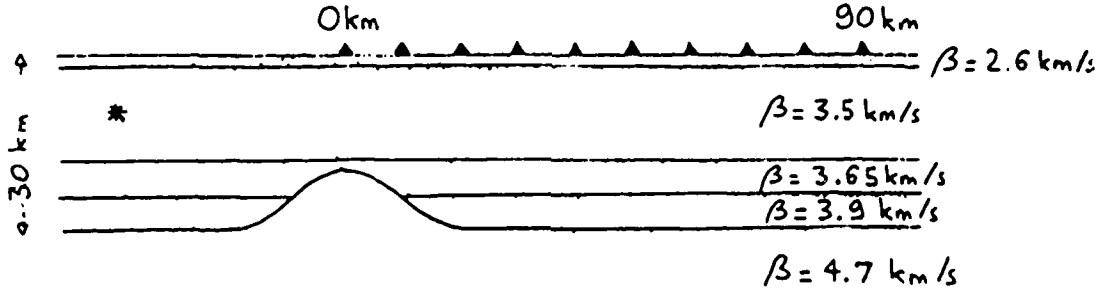

- Figure 1 -

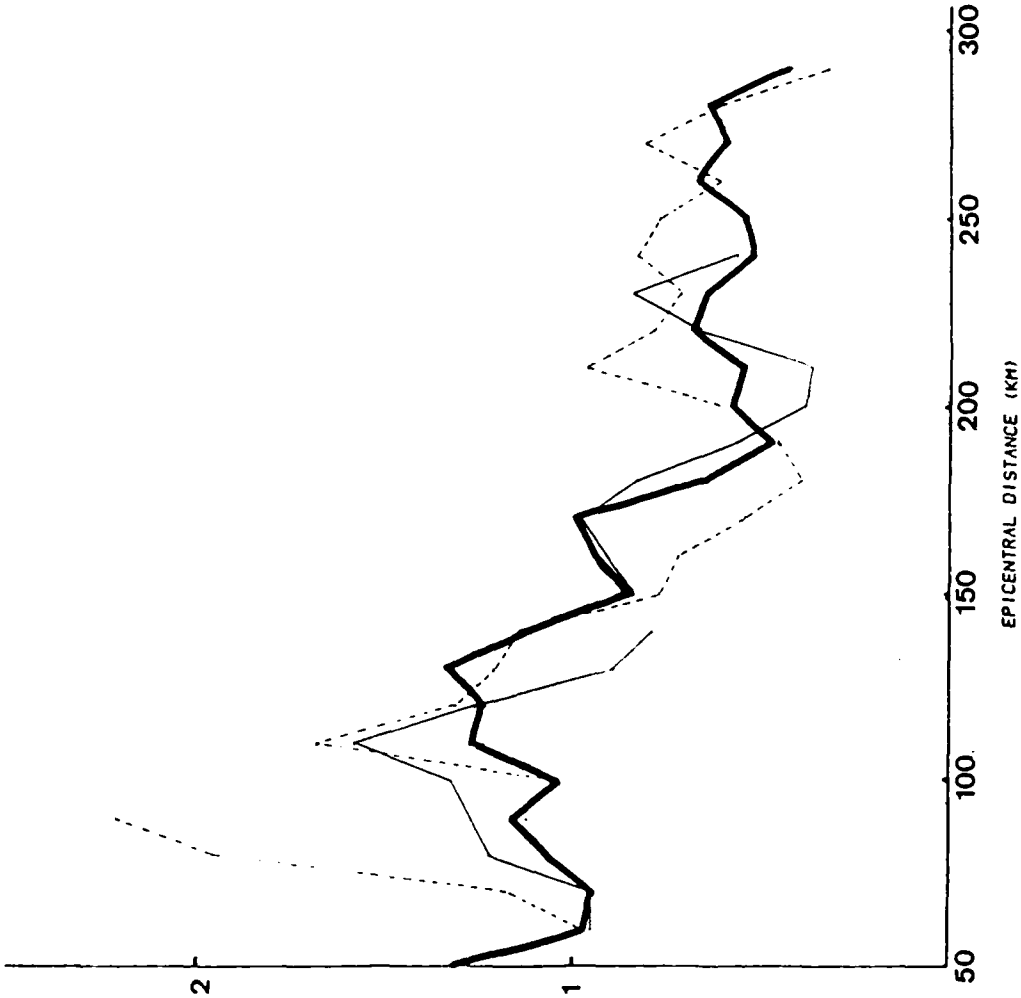

- Figure 2 -

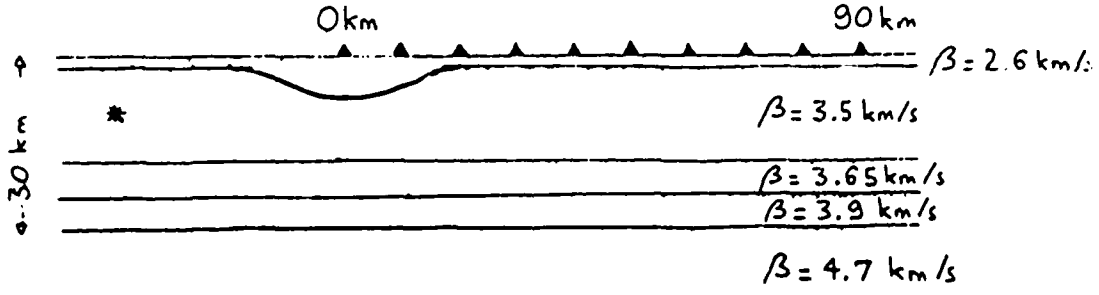

- Figure 3 -

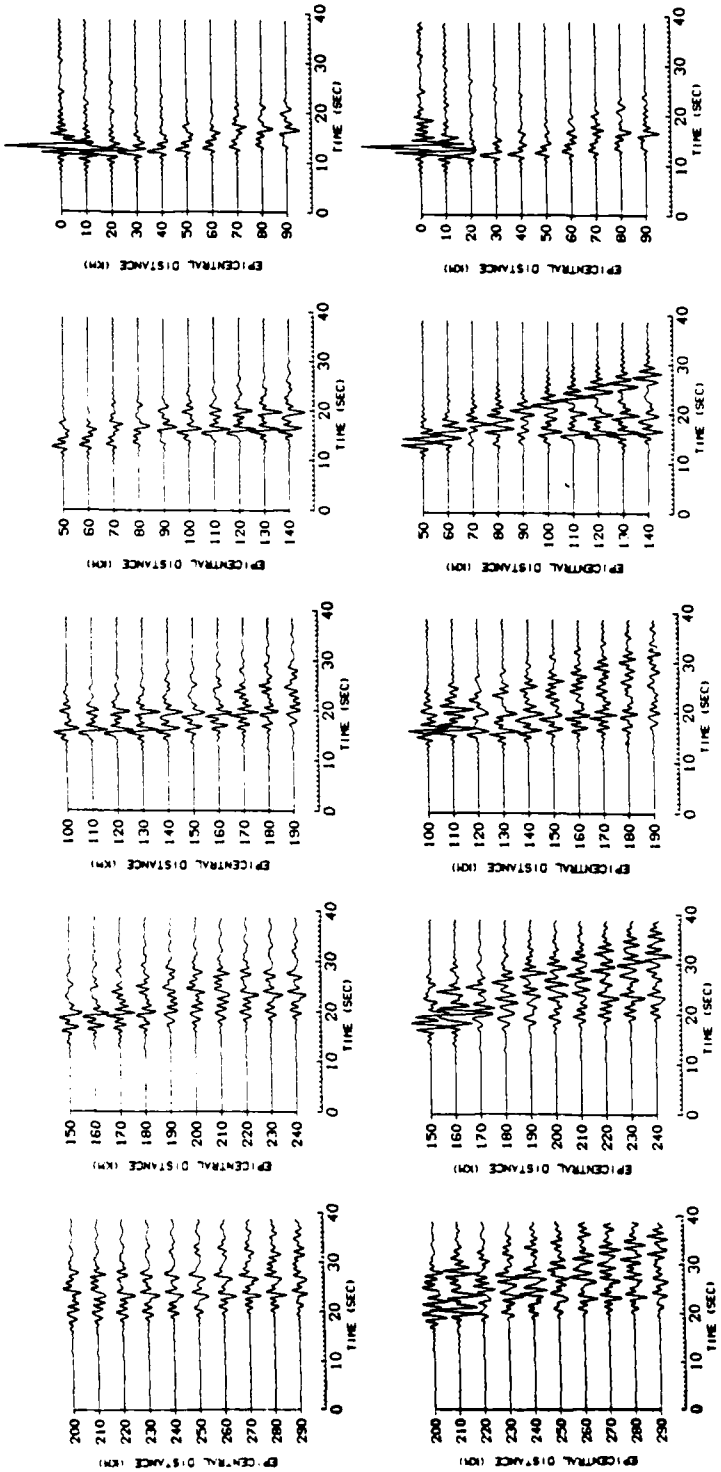

- Figure 4 -

AFGL/DARPA REVIEW OF NUCLEAR TEST MONITORING BASIC RESEARCH
U.S. AIR FORCE ACADEMY , 6-8 MAY 1986

DETERMINATION OF SOURCE FUNCTION FOR A SEISMIC SWARM

Pierre MECHLER - Florence RIVIERE
RADIOMANA

In despite of the title of this presentation, we will not present a study of source functions, but a way to obtain a signal averaged over the seismic stations of the French Seismic Network, which will enable us to study the source in a future work.

I. Obtention of the averaged signal.

A classical way of averaging signals over a seismic network is to use a "Delay and Sum". In this procedure, a simple stack of the various signals are done, without taking into account the change in the records of each station.To overcome this problem, we decide to define what we will call the best averaged signal in a least square sens.

The technic used is far from beeing new. We suppose each of the records to consist of:

- a common signal but multiplied by a station's factor.
- a noise (mostly wave generated) completely decorrelated from the common signal.

The signals are first suppossed to be delayed, so to be in phase, but we will come back later to this point. We compute the correlation matrix of all signals. It can be shown that the station's factors is one of the eigen vectors of this matrix, the one corresponding to the largest of all eigenvalues. This introduce an undetermination: an eigen vector is allways obtained up to a constant, but this is obvious on physical basis, it is possible to multiply the station's factors by an arbitrary number, if in the same time, the common signal is divided by the same value.

The common signal is then, the sum of the records, averaged by the just computed station's factors. The wave generated noise, or residual signal in a given station, is

obtained by a difference between the record in the station and the common signal.

This decomposition of the signals is quite similar to the covariance analysis, well-known in statistical studies. The main difference is that in statistics, the decomposition of the signals is usually done on a larger set of eigen vectors than just the first one. But, in our case, only the first as a meaning, corresponding to a signal beneath France and representing the source function filtered by the propagation. A decomposition on a larger set will have no physical meaning, the coda in each station, are only statisticaly similar. Of course, such a decomposition has to be done over a seimic network which aperture is small enough compared to the epicentral distance.

This procedure is relatively sensitive to the determination of the arrival time in each station. We were greatly helped in this by the origin of the events we studied. It consist in a "seismic swarm", a serie of very similar events from the same area in Eastern Kazakh, not far from Shagan River. The signals recorded in one station for the various events are more similar than the signals recorded in the stations of the French Seismic Network for the same event. So, in a first step, we computed the common signal in each single stations for a set of 10 events. It was easier to measure the arrival time on this averaged signal, then to obtain a precise arrival time for each record by a correlation technic. We also checked, by iteration, that it was not possible to improve the time determination.

We vary the length of the time window used in the computation. The samplig rate of our records is 50Hz, with an anti-aliasing filter at 16Hz, in fact all of our data were low-pass filtered at 8Hz. The various time windows were between 1024 points (about 20 seconds) and 128 points (2.5 seconds) without real change in the station's factors.

II. Magnitude determination.

The first interpretation is to consider the common signal, in the various stations, as representing the signal arriving beneath France and filtered by an average crust, the station's factors as a measure of the sensitivity of each station, and the residual signal as athe coda (in fact we obtain more than the coda, we also have energy in the beginning of the signal, see later).

We will start by magnitude considerations. We studied two different ways to measure the magnitude. In the first, for each station, we computed for all events a common signal and ,in that case, the event's factors. The magnitude beeing the logarithm of the wave amplitude, plus a distance correction, and as all events are practicaly at the same distance, the logarithm of the event's factors should be, within a constant correction, the event's magnitude.

Using the magnitude determination of the French Network, we found the best relation between magnitude and log of event's factor to be of the form:

$$mb = a*\log(EF) + b$$

but with a "a" factor not equal to 1. We give in annex the list of all the results, the mean values are:

$$a = 0.837 \quad +/-.086$$
$$b = 5.952 \quad +/-.035$$

We also used only nine of the events to recompute a and b , to calculate the magnitude of the last one. Volontarily, we select the nine smallest events to obtain the magnitude of the largest. The result were:

$$m = 6.17 \quad +/-.03$$

which is exactly the value found by the French Network.

We intent to apply the same technic, on a much larger data set, in order to obtain, not really a magnitude, but a classification of the various events, according to their energy.

This first way to determine a magnitude is rather tedious: each time a new event is aded to the data base, all computations have to be redone. An other way, is to use the mean station's factors. We noticed that the station' factors are very similar for a given station and the various events. So, we first computed an average value of the station's factor, in each station for all events, then we computed an approximation of the common signal, using this new set of station's factors and measured it's amplitude. The results are given in annex.

III. Source function.

The common signal, from all stations of the network and a given event, represents an approximation of the incoming signal, beneath France and filtered by the mean french crust. We present here some of the common signal we obtained. In this preliminary part of the work, we have not yet compare our results with a synthetic sismogramm, using a source function and a propagation effect.

In the following figures, we plotted the common signals for all ten events used in this study, and also, for comparison, the actual signals in some stations both for the best event and an average one.

IV. Signal residuals.

The difference between the actual record and the common signal represents more than the coda. As we pointed earlier, we also have energy in the first part of the signal.

In the figures, we show the mean signal computed using all events in the fives stations of Massif Central, in the middle of France. And, for the same stations, the mean residual signal.

On this last plot, some coherency between the signals accross the subarray is clearly seen.

We think that the size of the seismic network is an important parameter for the coherency of the waves accross it. If the aperture is too small, we expect to obtain a high coherency for the signals themselves (up to the amplitude which is known to varry), so the residual signals should represent the coda. If the aperture is larger, then it is possible to observe propagations through the array. We know, from other studies, that the crust, just south of the sub-array, presents larg anomalies. We whish to correlate both phenomens.

V. Preliminary conclusions.

This presentation is only a presentation of a current work. Our method for precise magnitude determination has already given us very good preliminary results, and we will improve our statistic by increasing the number of events.

The common signals, obtained for a given quake, over our network will allow a study of the source function. And we really hope to explain the main trends of the residual signals by correlation with the geological structure around the network.

Annex

Magnitude coef. with all events

a	b
0.7527	5.9658
0.8390	5.9690
0.8184	5.9445
0.7185	5.9974
0.8635	5.9124
0.7973	5.9924
0.8387	5.9021
0.8313	5.9924
0.9131	5.9124
0.7698	5.9687
0.8024	5.9529
0.9291	5.9509
0.8525	5.9552
0.8399	5.9574
0.8257	5.9629
0.8985	5.9497
0.8849	5.9441
0.8236	5.9285
0.8575	5.9212
0.8890	5.9227
0.8103	5.9494
0.8578	5.9210
0.8799	5.9135
0.8114	5.9365
0.7131	5.9693
1.1354	5.9337
0.6380	6.0732

Table I

Magnitude computed from common signal

$$m=a*\log(A)+b$$

a=0.886 b=6.406

29/03/81	5.49
13/09/81	6.20
31/08/82	5.34
26/12/82	5.60
20/11/83	5.36
06/10/83	6.03
07/03/84	5.52
10/02/85	5.69
29/03/84	6.00
14/07/84	6.18

Table II

Magnitude computed from station's factors

station	e0	e1	e2	e3	e4	e5	e6	e7	e8	e9
LBF	5.56	6.15	5.43	5.54	5.24	6.03	5.40	5.88	5.97	6.17
LOR	5.50	6.14	/	5.62	5.35	6.03	5.42	5.92	5.97	6.17
AVF	5.66	6.13	5.17	5.57	5.37	5.87	5.61	5.85	6.02	6.18
LSF	/	/	/	/	5.33	/	5.48	5.88	6.01	6.19
SSF	5.60	6.12	5.09	5.63	5.43	5.91	5.65	5.90	5.97	6.12
MFF	/	6.15	5.44	5.50	5.26	6.02	/	5.91	5.98	6.17
GRR	/	/	5.17	5.63	5.39	5.92	5.62	/	5.97	6.15
FLN	/	6.20	5.31	5.58	5.33	5.94	5.47	/	6.02	6.17
LDF	/	/	5.24	5.61	5.37	5.95	5.51	/	6.01	6.17
SMF	5.63	6.19	5.39	5.52	5.28	/	5.42	5.87	5.98	6.17
LRG	5.67	6.16	5.20	5.57	5.33	5.85	5.59	5.85	6.02	6.18
TCF	/	6.17	5.25	5.64	5.29	5.98	5.55	5.93	5.98	6.13
RJF	5.63	6.18	5.26	5.54	5.34	5.92	5.48	5.87	6.02	6.18
FRF	5.63	6.17	5.30	5.53	5.31	5.93	5.47	5.91	5.99	6.19
LPO	5.61	6.17	5.30	5.53	5.34	5.95	5.45	5.87	6.00	6.19
LFF	5.58	6.18	5.26	5.56	5.34	5.96	5.48	5.88	5.99	6.18
EPF	5.59	6.16	5.24	5.57	5.36	6.05	5.49	5.82	5.96	6.17
BSF	5.60	6.11	5.14	5.59	5.38	5.96	5.58	5.93	6.00	6.13
HAU	5.62	6.16	5.20	5.58	5.36	/	5.50	/	5.98	6.16
CDF	5.55	6.17	5.15	5.65	5.37	/	5.60	5.90	5.97	6.10
LMR	5.64	6.13	5.22	5.53	5.31	5.94	5.57	/	6.04	6.15
LPF	/	/	5.23	5.59	5.37	5.92	5.56	5.87	6.02	6.19
CAF	/	/	5.25	5.62	5.34	5.99	5.50	/	5.99	6.16
MZF	/	/	5.30	5.53	5.34	5.93	5.53	5.89	6.03	6.19
CVF	/	/	/	5.57	/	5.96	5.54	5.88	6.01	6.18
BGF	/	/	/	/	5.27	/	5.55	5.91	5.98	6.17
HYF	/	/	/	/	/	/	/	5.90	6.00	6.18
mean	5.60	6.16	5.24	5.58	5.34	5.95	5.52	5.89	5.99	6.17
sig	0.04	0.02	0.09	0.04	0.04	0.05	0.06	0.02	0.02	0.02
LDG	5.5	6.18	5.3	5.6	5.3	5.96	5.5	5.89	6.02	6.17

Table III

Figures Caption

Fig 1 : common signals for the ten events of this study

Fig 2 : Actual signals for event 1 : 13/09/81

Fig 3 : Actual signals for event 4 : 20/11/83

Fig 4 : Averaged records in the 5 stations of Massif Central

Fig 5 : Averaged residual signals in the 5 stations of Massif Central

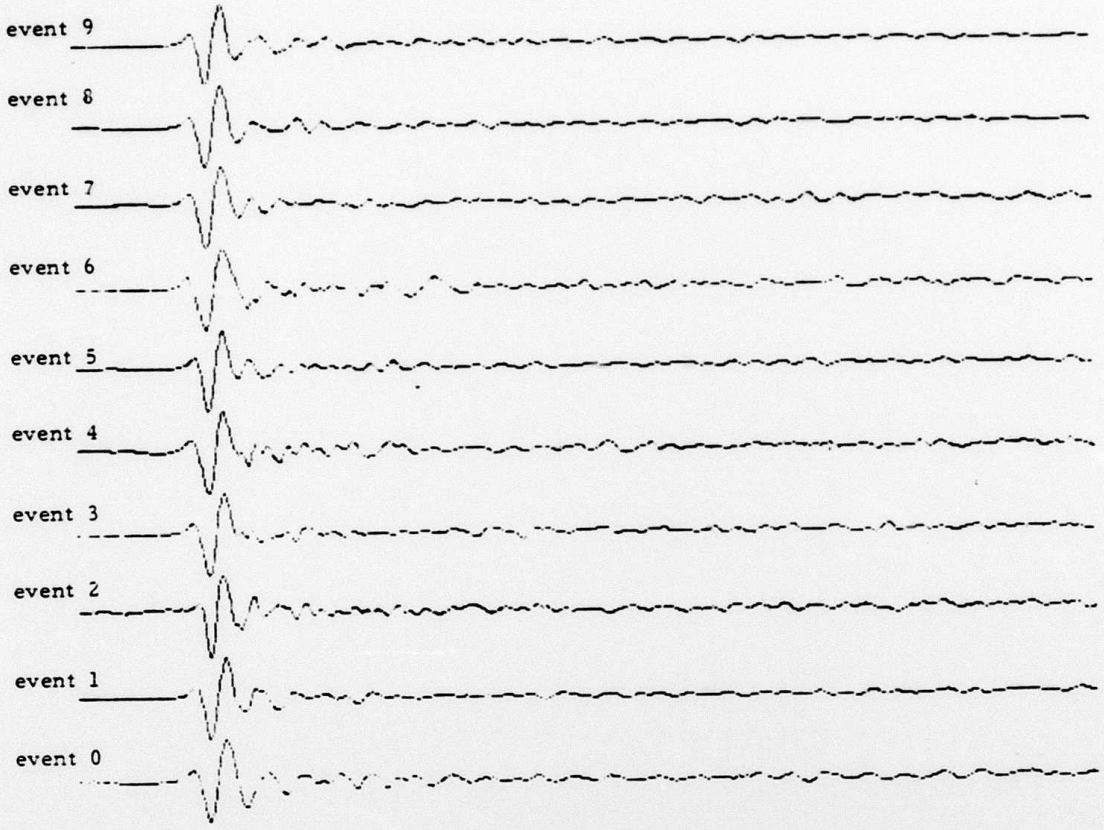
event 9
event 8
event 7
event 6
event 5
event 4
event 3
event 2
event 1
event 0

Fig 1

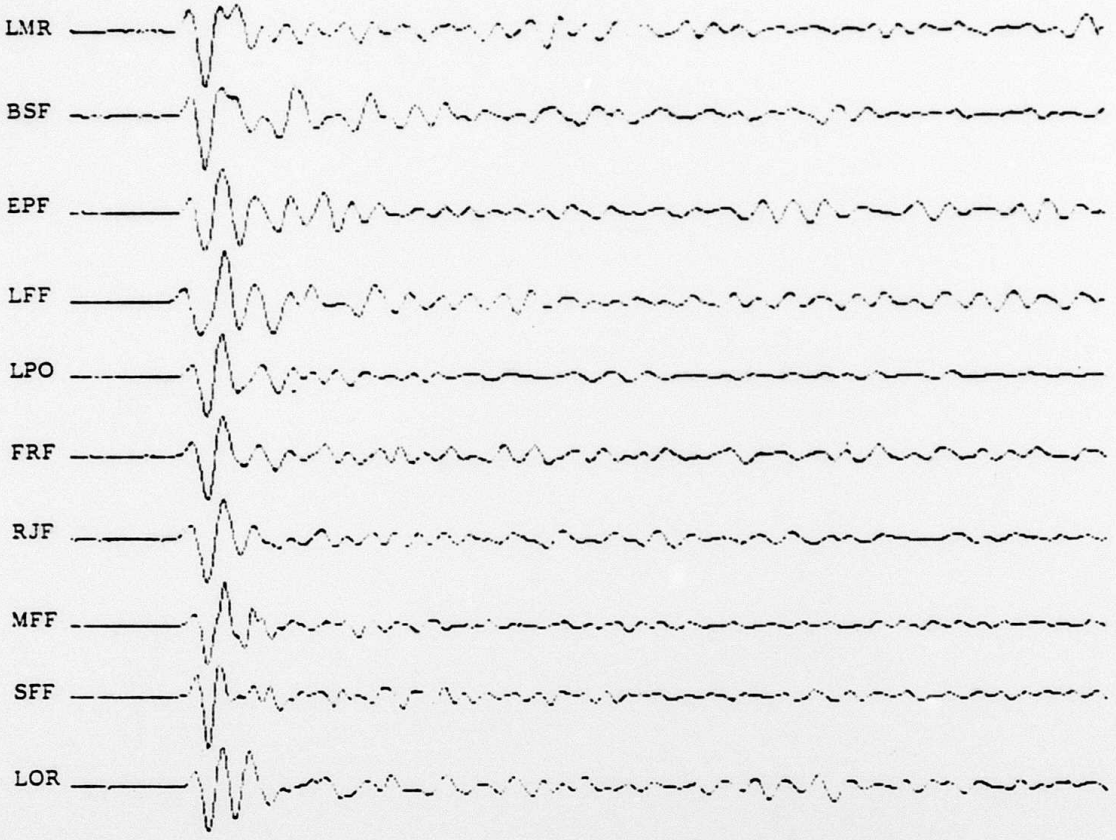

Fig 2

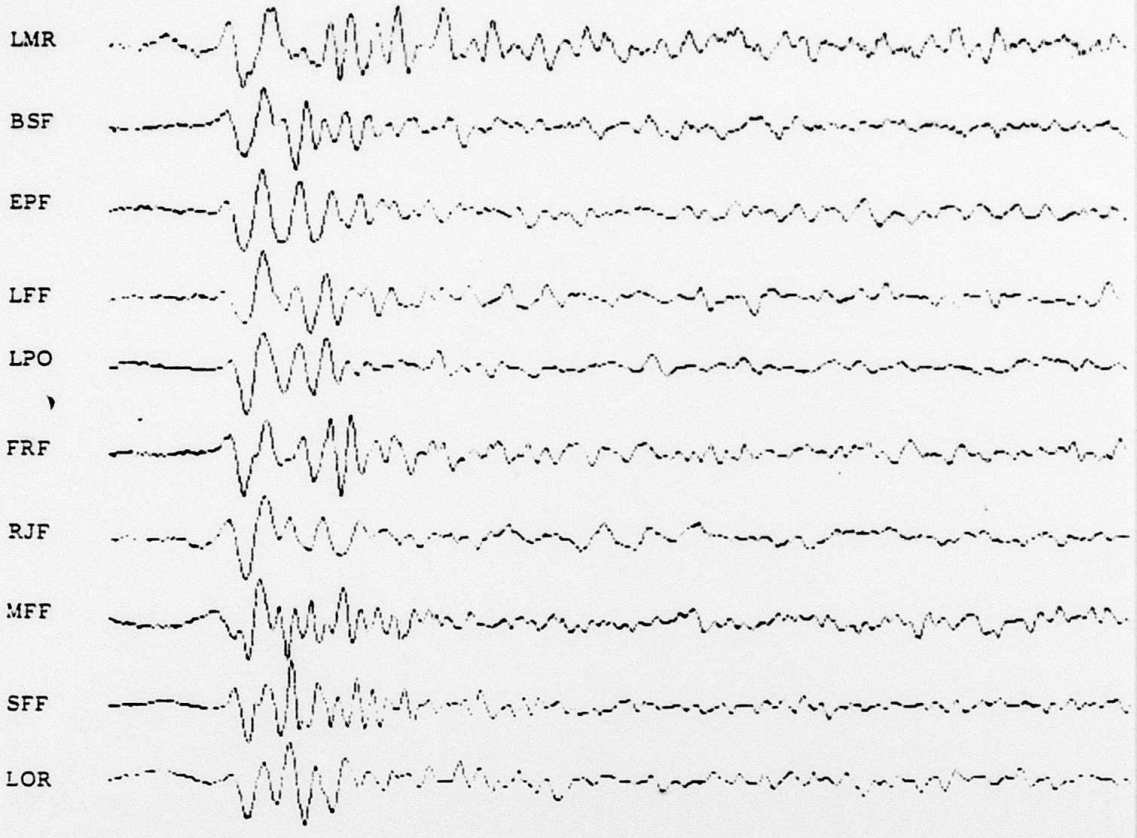

Fig 3

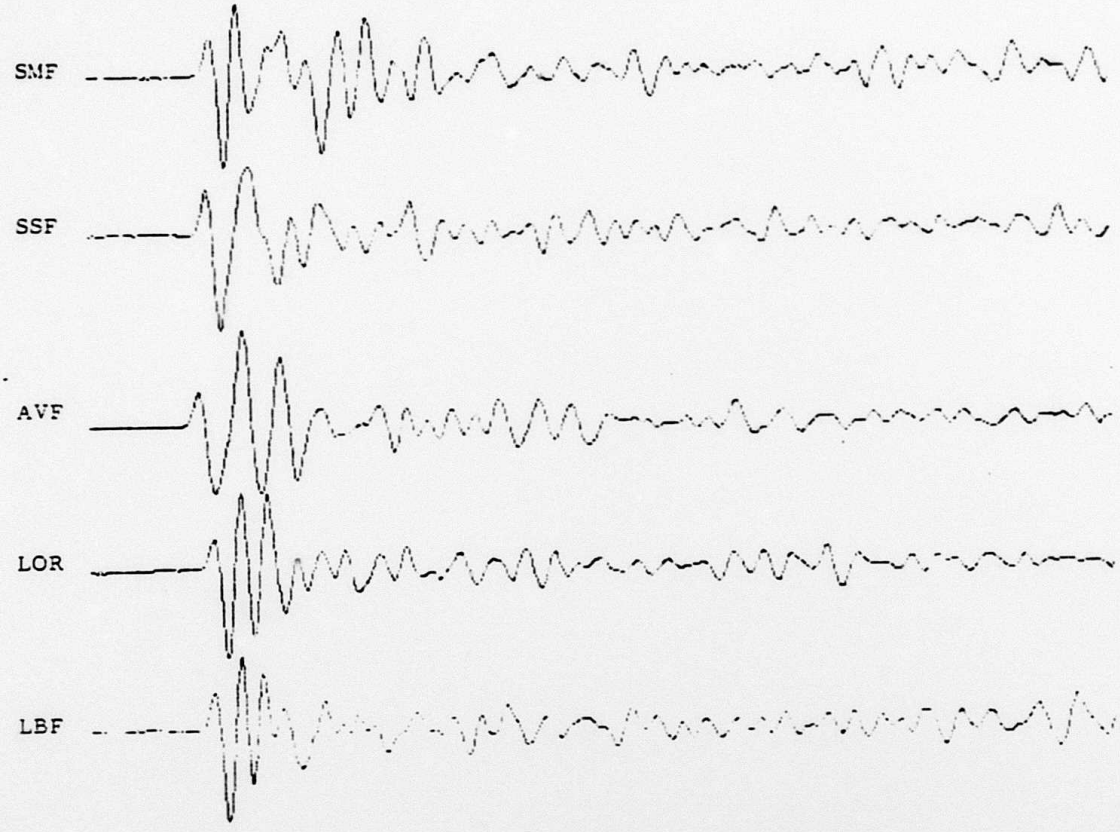

Fig 4

Fig 5

AFGL / DARPA Seismic Research Symposium

U. S. Air Force Academy

Colorado Springs - 6 - 8 May 1986

Paper tittle : Regional Distribution of apparent attenuation in the Center of France

Paper authors : M. Campillo - Radiomana

Grant n° 85 0033

The set of seismic data is the one already used in our previous studies on Lg waves (18 quakes with ML between 3.2 and 4.8, within the crust; 22 SP stations of the LDG network).

The method used here is the Algebric Reconstruction Technic (ART) to build up an image of the Q factor spatial distribution.

The set of propagation paths is presented in Figure 1.
Each point of the image of Q_o takes into account all the paths within a distance of 50 km.
In order to apply some confidence criterium on the quality of this Q evaluation we define a confidence index :

$$i_c = n_{source} \times l_{rays}$$

where :

n_{source} : is the numbers of different sources which generate the rays

l_{rays} is the length of the ray inside the influence circle divided by the influence radius.

A map of this index is given in Figure 2, where the represented points fit the test of ray length.

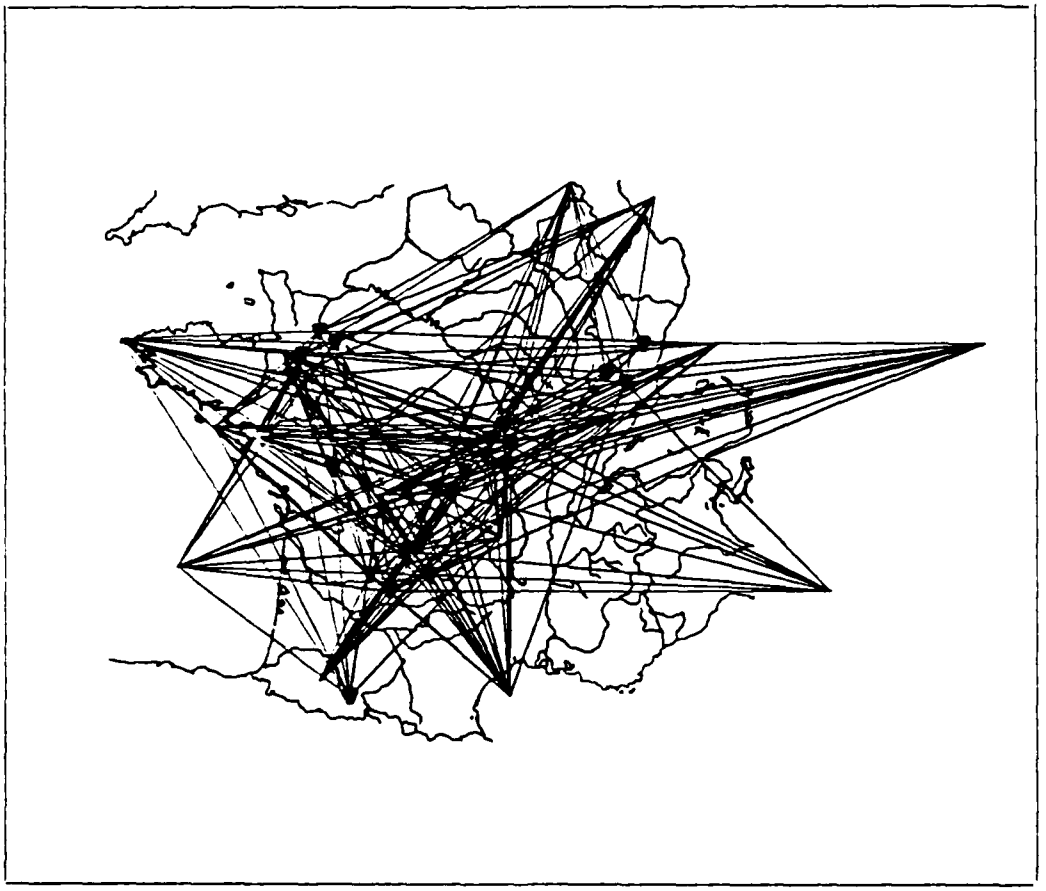

Figure 1

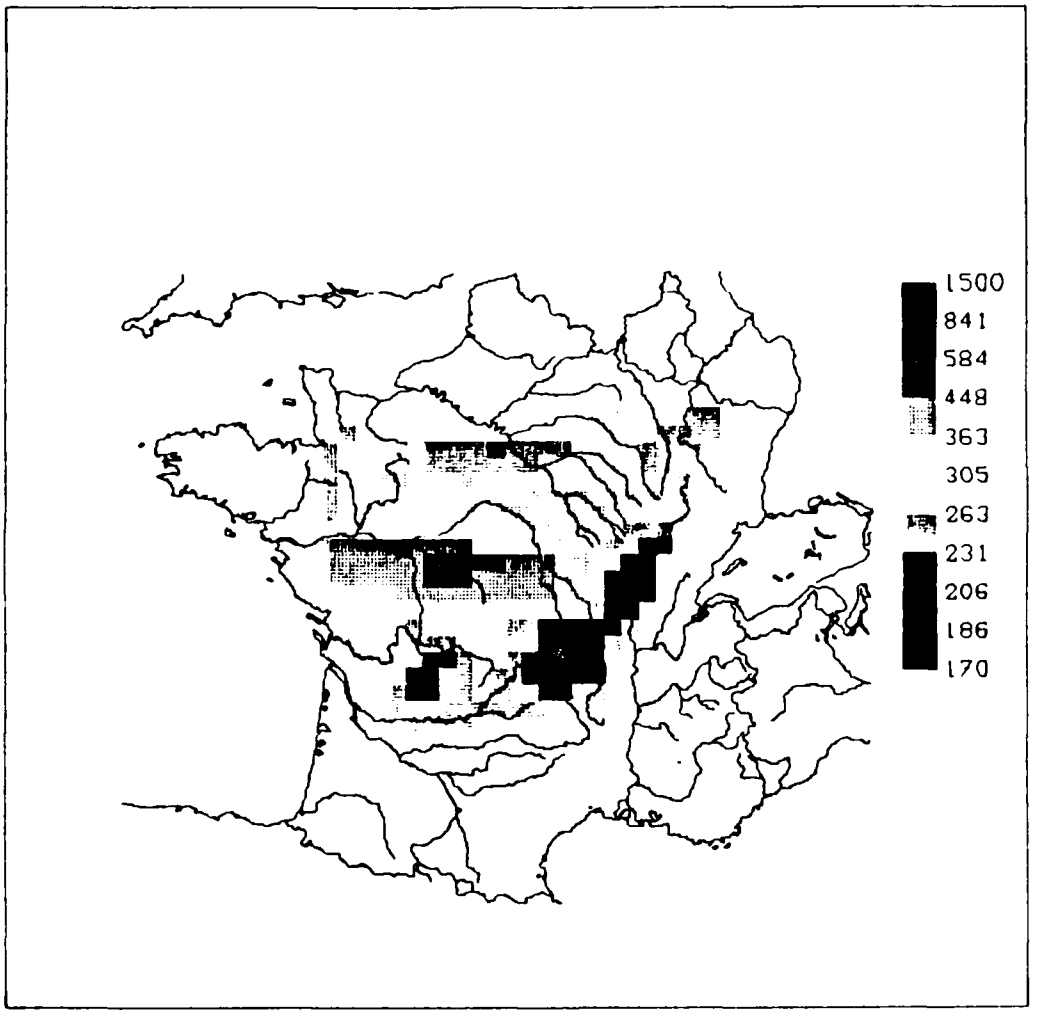

Figure 2

As a result, all the blue zones correspond to a high confidence index, and red zones might include systematic bias.
Figure 3 represents a rather simple regional distribution. If one just keeps within high confidence limits, the main regions are defined as :
- Limagne Basin , Forez, Saone valley = weak figure for Q
(between $Q_\circ$ = 180 and $Q_\circ$ = 240)
- Limousin = (between $Q_\circ$ = 200 and $Q_\circ$ = 260)
- South Parisian basin, Berry, Poitou, North of Massif Central
(between $Q_\circ$ = 300 and $Q_\circ$ = 440).

The mean $Q_\circ$ value (always computed at f = 1 Hz) extracted from these results is : $Q_\circ$ = 290
Similar to the one obtained by direct Lg measurement (Campillo and al 1984).
We need to extend this $Q_\circ$ cartography to other western Europe regions by using other stations and earthquakes.

Conclusion

These results pointed out the importance of graben zones for Lg waves propagation. Nevertheless, at this stage of the study we do not possess yet any separation tool between two types of phenomena which could create attenuation :
- small scale diffraction (or scattering)
- large scale geometrical effect
A study of frequency dependancy for Q should help us in the interpretation of our data.
On the other hand, developpements of numerical simulation methods encourage us to investigate more complex zones in order to interprete the quasi extinction phenomena of Lg waves we have observed along peculiar paths.

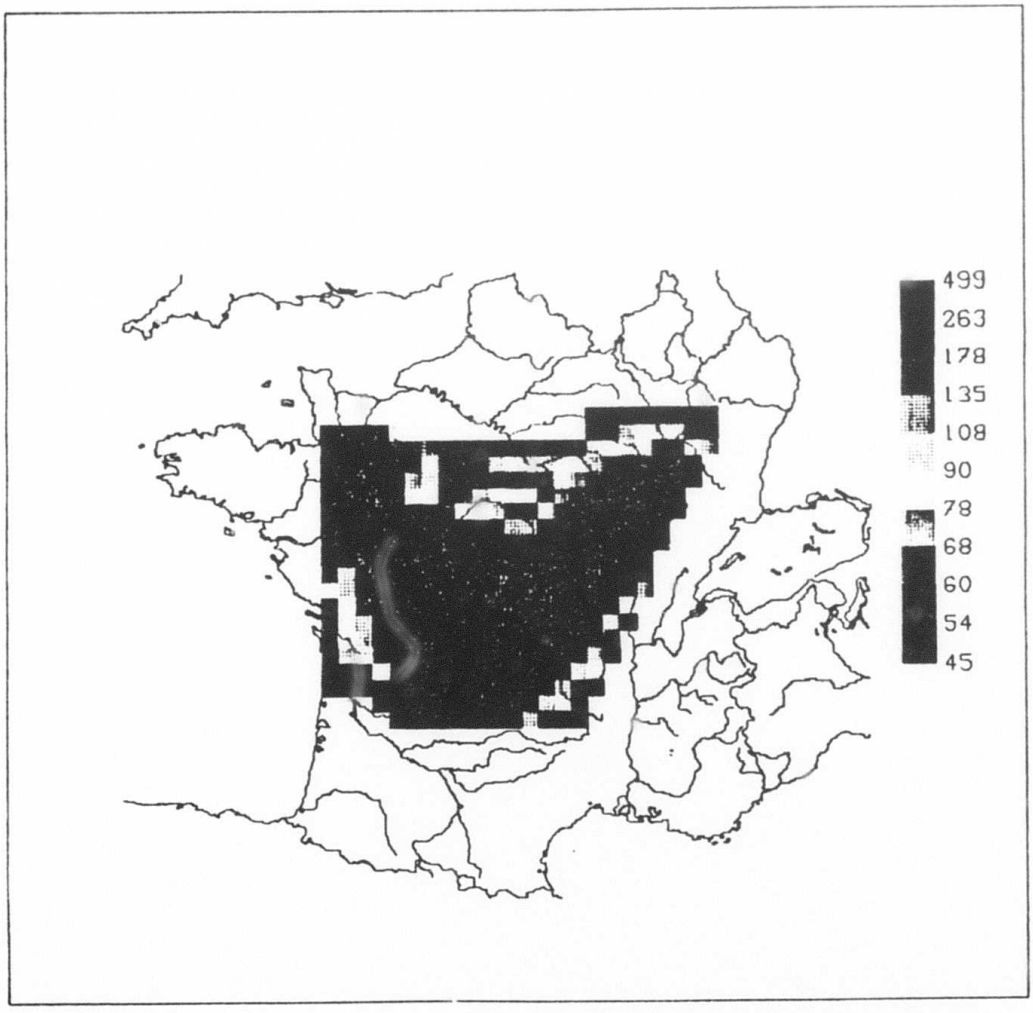

Figure 3